Geochemistry Geophysics Geosystems G3
AN ELECTRONIC JOURNAL OF THE EARTH SCIENCES
Published by AGU and the Geochemical Society

*Article*
Volume 2
September XX, 2001
Paper number 2000GC000100
ISSN: 1525-2027

# Geodetic constraints on postseismic deformation following the 1990 $M_s$ 7.8 Luzon earthquake and implications for Luzon tectonics and Philippine Sea plate motion

**John Beavan**
Institute of Geological and Nuclear Sciences, PO Box 30-368, Lower Hutt, New Zealand (j.beavan@gns.cri.nz)

Also adjunct at Lamont-Doherty Earth Observatory of Columbia University, Palisades, New York 10964, USA

**David Silcock**
School of Geoinformatics, Planning and Building, University of South Australia, Adelaide, South Australia 5001, Australia

Now at Department of Geospatial Science, RMIT University, GPO Box 2476V, Melbourne, Victoria, Australia (David.Silcock@rmit.edu.au)

**Michael Hamburger**
Department of Geological Sciences, Indiana University, Bloomington, Indiana 47405, USA (hamburg@indiana.edu)

**Emmanuel Ramos**
Philippine Institute of Volcanology and Seismology, C. P. Garcia Avenue, U.P. Campus, Diliman, Quezon City, Philippines (eramos@phivolcs.dost.gov.ph)

**Catherine Thibault**
Department of Geological Sciences, Indiana University, Bloomington, Indiana 47405, USA (cthibaul@bellsouth.net)

Now at Chevron, 935 Gravier Street, New Orleans, Louisiana 70112, USA

**Renato Feir**
National Mapping and Resource Information Agency, Manila, Philippines

[1] **Abstract:** We have obtained three epochs of high-quality dual-frequency GPS data at 15 stations in the Luzon, Philippines, region since the July 16, 1990, $M_s$ 7.8 earthquake, from which we generate horizontal velocity fields at the Earth's surface for the 1993–1996 and 1996–1998 periods. We use these velocities, plus 1996–1998 GPS velocity results reported elsewhere from 13 additional stations, to show that present-day deformation in Luzon is dominated by strike-slip motion along the Philippine fault system. The measured strike-slip rate across central Luzon is faster than the expected long-term slip rate on the fault, which we attribute to postseismic deformation following the 1990 earthquake. The 1993–1996 and 1996–1998 deformation patterns cannot be statistically distinguished within the ~10% uncertainties of the data. If the observed deformation is interpreted using an elastic half-space model with uniform slip below a subsurface locking depth, we find a fault slip rate of 40 mm/yr and a locking depth of ~15 km. This is too fast to be a steady interseismic rate, as it disagrees with what is known from paleoseismic and other evidence about earthquake recurrence and long-term slip rate on the Philippine fault system in

central and northern Luzon. Also, a 15 km locking depth for steady interseismic slip is probably too shallow compared to the depth of rupture in the 1990 earthquake. If the deformation is instead interpreted with two types of viscoelastic model, we find that the observed velocities can be fit well for a range of values of lower lithosphere viscosity and long-term slip rate. Using a two dimensional (2-D) viscoelastic coupling model, the minimum allowable lower lithosphere viscosity is $0.5 \times 10^{19}$ Pa s, with an associated long-term slip rate of 15–22 mm/yr. Faster long-term slip rates also fit well, with correspondingly higher values of viscosity. With a possibly more realistic model that includes 3-D viscoelastic effects we find preferred long-term velocities in the range 20–35 mm/yr and viscosities in the range $2–6 \times 10^{19}$ Pa s. Our preferred viscosities correspond to Maxwell times on the order of 7–20% of the typical earthquake recurrence interval and are several times higher than values found for a number of Californian strike-slip earthquakes. Other implications of our 1993–1998 surface velocities are that the Philippine Sea-Eurasia (PH-EU) Euler vector of *Seno et al.* [1993] is a better description of the PH-EU convergence rate than a Euler vector recently estimated from GPS velocities in the northern PH and that the great majority of the normal component of PH-EU plate convergence is taking place west of Luzon, presumably largely at the Manila Trench. We also find that Luzon is rotating counterclockwise relative to PH at 1°–2°/Myr, only ~25% of the rate recently suggested by other workers on the basis of limited GPS data.

**Keywords:** Luzon earthquake; Philippine fault; postseismic deformation; crustal rheology; Philippine plate motion.

**Index terms:** Crustal movements-interplate; plate boundary-general; plate motions-present and recent; rheology-crust and lithosphere.

**Received** August 24, 2000; **Revised** May 3, 2001; **Accepted** July 1, 2001; **Published** September XX, 2001.

Beavan, J., D. Silcock, M. Hamburger, E. G. Ramos, C. Thibault, and R. Feir, 2001. Geodetic constraints on postseismic deformation following the 1990 $M_s$ 7.8 Luzon earthquake and implications for Luzon tectonics and Philippine Sea plate motion, *Geochem. Geophys. Geosyst.*, vol. 2, Paper number 2000GC000100 [16,950 words, 8 figures, 9 tables]. Published September XX, 2001.

## 1. Introduction

[2] The Philippine Islands form part of the complex boundary between the Philippine Sea (PH) and Eurasian (EU) Plates (Figure 1). In the central and southern Philippines most of the deformation is partitioned between approximately trench-normal westward directed subduction at the Philippine Trench and left-lateral strike-slip motion on the intra-arc Philippine Fault [*Fitch*, 1972; *McCaffrey*, 1996]. Both the trench and the fault are quite recent, with their activity beginning between 2 and 4 Ma [*Cardwell et al.*, 1980; *Aurelio et al.*, 1991; *Barrier et al.*, 1991]. At the latitude of Luzon the east dipping Manila Trench to the west of Luzon has been the primary plate boundary since the late Miocene [*Karig*, 1973; *Murphy*, 1973], but it does not presently show high levels of seismic activity [*Cardwell et al.*, 1980]. It has been proposed [*Fitch*, 1972; *Karig*, 1973] that subduction east of the Philippine Islands is propagating northward along the East Luzon Trough, which is connected to the Philippine Trench by a left-lateral trench-trench transform and which will eventually take over from the Manila Trench as the primary plate boundary. This hypothesis has been most thoroughly investigated by *Lewis and Hayes* [1983], who suggest that the incipient subduction along the East Luzon Trough is reactivating a Tertiary subduction zone. *Hamburger et al.* [1983] find some evidence for ongoing convergence between PH and northeastern Luzon in a series

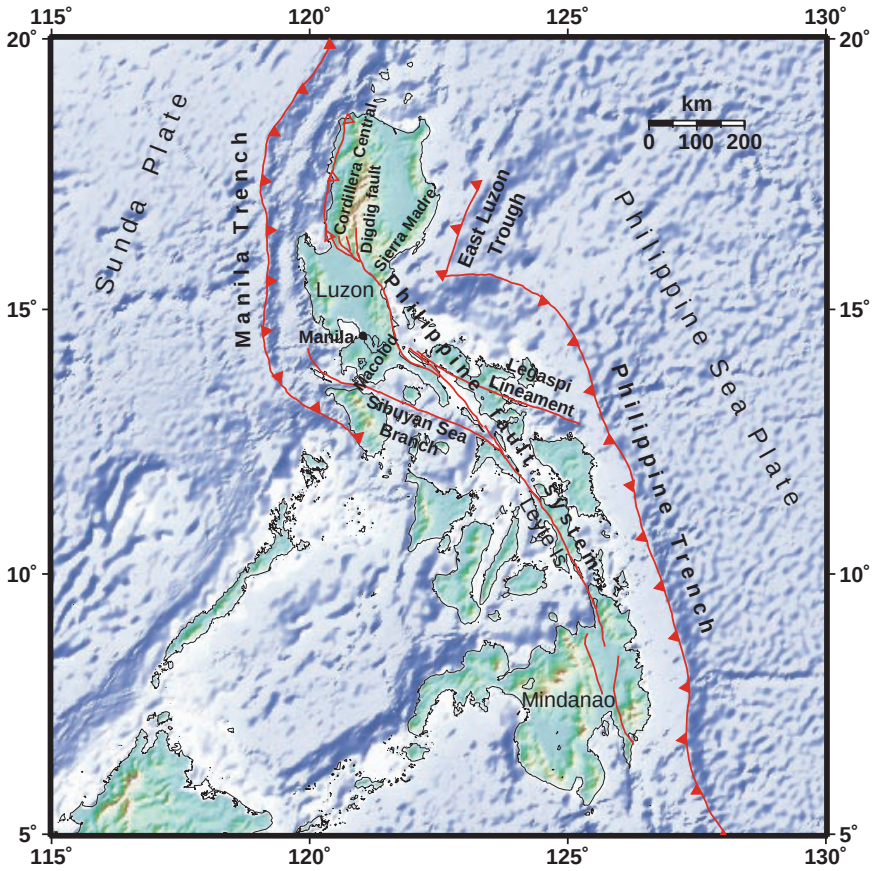


**Figure 1.** Major tectonic features of the Philippine region relevant to this study, shown on a background of shaded relief topography and bathymetry lit from the southeast. Faults with solid triangles are active and possibly active subduction zones. The fault shown with open triangles in western Luzon is the active convergence zone of *Barrier et al.* [1991]. The Philippine fault system is a predominantly left-lateral system that splits into several splays in central Luzon. (*Rangin et al.* [1999] call the section of the Philippine fault system that failed in the 1990 earthquake the Infanta Fault, rather than the Philippine Fault/Digdig Fault terminology we use here.) The "Sunda Plate" (comprising southeast Asia and the South China Sea) is moving as much as 10–15 mm/yr east or southeast relative to stable Eurasia [*Michel et al.*, 2001] (see also Table 4).

of large thrust-type earthquakes that occurred along the trough between 1968 and 1977. However, there is presently no evidence for active subduction north of 17°–18° at the East Luzon Trough [*Bowin et al.*, 1978; *Cardwell et al.*, 1980; *Hamburger et al.*, 1983; *Lewis and Hayes*, 1983, 1989], so that the present convergence rate across the trough cannot be very rapid. Supporting this, *Hamburger et al.* [1983] find no marine geophysical evidence for substantial recent slowing of subduction at the Manila Trench. It is thought that the ongoing reorganization of plate boundaries in the Luzon region is related to the island arc–continent collision in Taiwan, which began at ~5 Ma [*Karig*, 1973; see also *Hall*, 1996].

### 1.1. Philippine Fault

[3] The nature of the Philippine Fault as one of the world's great continental strike-slip faults was first properly recognized by *Allen* [1962],

but its long-term slip rate and earthquake recurrence history remain relatively poorly known. A number of large earthquakes have been relocated close to the Philippine Fault [*Rowlett and Kelleher*, 1976], suggesting that it is currently active through most of its length.

[4] The left-lateral slip rate on an apparently creeping section of the fault near 11°N on Leyte Island has been measured using detailed GPS surveys at 26 ± 10 mm/yr [*Duquesnoy et al.*, 1994], and this rate has been refined to 35 ± 4 mm/yr with the collection of additional data (*Dusquenoy* [1997], quoted by *Rangin et al.* [1999]). These results add to the evidence of slip partitioning between the Philippine Fault and Philippine Trench.

[5] Farther north, the situation becomes more complex. The primary locus of subduction appears to transfer from the Philippine Trench in the east to the Manila Trench in the west. Major structures, the Legaspi Lineament and the Sibuyan Sea Branch, intersect the Philippine Fault from the east and west, respectively (Figure 1). These are each interpreted by various authors to carry on the order of 10 mm/yr left-lateral slip [e.g., *Bischke et al.*, 1990; *Aurelio et al.*, 1998]. The presence of an extensional region, the Macolod Corridor, situated to the southwest of the Philippine Fault in southern Luzon, implies that the slip rate on the fault north of the corridor should be less than that to the south [e.g., *Rangin et al.*, 1999].

[6] *Rangin et al.* [1999] use limited GPS data from widely separated points in the Philippines to infer a predicted motion of 48 mm/yr in azimuth 280° across the Philippine fault system near 14°N in the southernmost part of Luzon Island, south of the Macolod Corridor. This resolves to ~39 mm/yr left-lateral slip as well as a significant thrusting component. However, there are no measurements directly across the fault system to confirm this estimate.

[7] In central and northern Luzon Island there is subduction to the west of the island at the Manila Trench and apparently active convergence to the east at the East Luzon Trough, though this activity decreases to the north as the trough dies out [*Hamburger et al.*, 1983]. The Philippine fault system separates into several splays, including the more northerly trending Digdig Fault, in the northern half of the island (Figure 1).

### 1.2. Slip Rates on the Philippine Fault in Central Luzon

[8] Prior to the 1990 $M_s$ 7.8 earthquake, only one large historical earthquake, the 1973 Ragay Gulf event well to the south, had been unequivocally associated with the Philippine Fault in Luzon [*Morante and Allen*, 1973; *Morante*, 1974]. Using historical records, geomorphological expression, and radiocarbon ages of wood in offset terraces, *Hirano et al.* [1986] estimate that the most recent historical earthquake to have broken the central Luzon section of the Philippine Fault occurred in 1645. It is believed that the historical record in the region is complete since 1645 for events higher than Intensity MM 7 [*Daligdig*, 1997], so it is unlikely that there have been intervening major events on this section of the Philippine Fault. Paleoseismic investigations, including trenching, of the Digdig and Philippine Faults subsequent to the 1990 quake [*Daligdig*, 1997] provide the most recent information on slip rate and earthquake recurrence interval. *Daligdig* [1997] finds evidence for six or seven past events on the fault sections that broke in the 1990 earthquake. Radiocarbon dating of the two events prior to 1990 provides good evidence to identify the 1645 earthquake with this fault segment and places the previous event in the range 1190–1390 A.D. *Daligdig* [1997] estimates from the trenching studies that the average earthquake recurrence interval on the Digdig Fault is

300–400 years, with a long-term slip rate of 9–17 mm/yr. He also notes that most estimates, by other authors, of slip rate based on faulted rock units and geomorphic data place the rate in the range 6–25 mm/yr, both on the Digdig Fault and on the Philippine Fault to the south. The most convincing of *Daligdig*'s [1997] new geomorphic estimates is based on a carbon-dated stream offset near the 1990 epicenter and gives a rate of 15 ± 3 mm/yr.

### 1.3. The 1990 Luzon Earthquake

[9] The 1990 Luzon earthquake was one of the largest continental strike-slip earthquakes of the twentieth century [*Yoshida and Abe*, 1992]. It caused observed ground rupture along 110 km of the Philippine Fault and one of its northern splays, the Digdig Fault, with 5–6 m of predominantly left-lateral surface offset [*Abe*, 1990; *Nakata et al.*, 1990, 1996; *Newhall et al.*, 1990] (Figure 2). The most reliable hypocentral depth is estimated from pP-P phases as 25 ± 0.9 km by the *International Seismological Centre* [1992]. Mapping of the surface rupture ended near Kayapa (Figure 2) because of difficulties of access to the mountainous terrain of the Cordillera Central farther north [*Nakata et al.*, 1996]. However, distributed aftershocks indicate that the rupture could have continued a further 50–100 km north [*Newhall et al.*, 1990]. Using centroid moment tensor inversion of long-period surface waves, *Yoshida and Abe* [1992] estimate the scalar moment of the earthquake as $3.9 \times 10^{20}$ Nm using a constrained centroid depth (i.e., the depth is not determined from the data) of 10 km, while the Harvard catalog gives $4.1 \times 10^{20}$ Nm using a constrained depth of 15 km. *Yoshida and Abe* [1992] estimate the fault length, width, and average slip as 120 km, 20 km, and 5.4 m, respectively, with nearly pure left-lateral strike-slip motion on a nearly vertical fault. Their estimate of 20 km fault width is based on the fact that almost all well-located aftershocks are shallower than 20 km [*Newhall et al.*, 1990; *Yoshida and Abe*, 1992]. *Silcock and Beavan* [2001] invert single-frequency GPS geodetic observations before and after the earthquake to find 5.5–6.5 m left-lateral slip along the mapped rupture and ~4 m oblique slip on a 40–50 km fault extension north of the mapped rupture. They find a relatively deep 20 km depth of faulting in the central 50–60 km of the rupture, with 12–15 km deep rupture toward the ends.

[10] In this paper we present evidence from GPS geodetic measurements that northeastern Luzon is moving at close to the Philippine Sea Plate rate and that the Philippine Sea-Eurasia (PH-EU) Euler vector of *Seno et al.* [1993] may slightly underestimate the PH-EU convergence rate but is nevertheless more realistic than a Euler vector determined recently from space geodetic data collected in the northern half of the Philippine Sea Plate [*Kotake et al.*, 1998]. We find that the left-lateral strike-slip rate on the Philippine fault system in Luzon has been close to 40 mm/yr between 1993 and 1998. This observed rate is higher than the long-term rate expected from paleoseismic and tectonic considerations and is probably in part a viscoelastic response to the 1990 earthquake. We use this interpretation to place limits on the viscosity of the lower lithosphere. We find that the surface deformation field in Luzon is not consistent with rapid (5.5°/Myr) counterclockwise rotation of Luzon relative to PH as has recently been suggested by *Rangin et al.* [1999], though we do find moderate 1°–2°/Myr counterclockwise rotation of Luzon relative to PH.

## 2. GPS Observations and Processing

### 2.1. GPS Data

[11] Our Philippine Islands Crustal Motion Project (PICMP) GPS data are summarized in Table 1. The April 1993 survey took place in

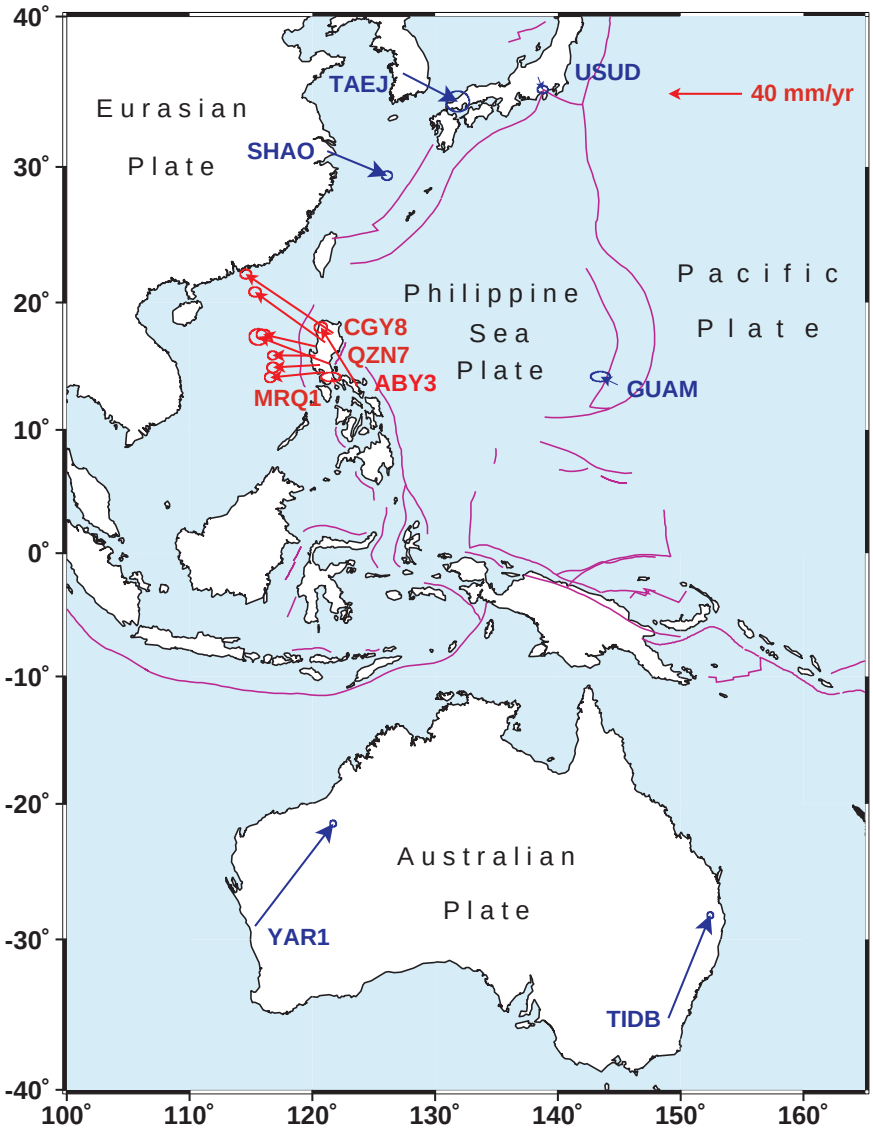


**Figure 2.** Velocities in the ITRF96 reference frame of the IGS stations we used to define the reference frame (thick blue arrows), plus the velocities in this frame of a selected subset of our stations (thin red arrows). In this figure, we do not differentiate the proposed Sunda and Amurian Plates from the Eurasian Plate.

two parts. The first consisted of 10 stations distributed nationwide designed (1) to provide a base network for future countrywide deformation studies and (2) to enable an earlier 1989–1990 survey using single-frequency GPS receivers to be adjusted onto a high-precision backbone and thus to improve its accuracy (D. M. Silcock, GPS technology to study crustal motions in the Philippine region, thesis in preparation, 2001) (hereinafter referred to as Silcock, thesis in preparation, 2001). The second part was a regional survey of 15 sites in Luzon, 10 of which had been observed in the 1990 postearthquake survey [*Silcock and Bea-*

**Table 1.** Numbers of Sessions Observed During Each GPS Campaign[a]

| NAMRIA Station | GPS ID | PICMP93[b] | PSP94[b] | PICMP96 | PICMP98 |
|---|---|---|---|---|---|
| ABY03 | ABY3 | 12 | 3 | 4 | - |
| ABY03 RM 4 | ABX3 | - | - | - | 1 |
| ARA01 | ARA1 | 2 | - | - | - |
| Magnetics 1995 Baler | ARX1 | - | - | 1 | 2 |
| BLN04 | BLN4 | 3 | - | 3 | 1 |
| CGY08 | CGY8 | 12 | - | 6 | 2 |
| CTN01 | CTN1 | 6 | - | - | - |
| IFG01 | IFG1 | 5 | - | 2 | 2 |
| ILN01 | ILN1 | 6 | - | - | - |
| ILO01 | ILO1 | 6 | - | - | - |
| LUN01 | LUN1 | 5 | - | 2 | 2 |
| LYT08 | LYT8 | 5 | - | - | - |
| MMA01 | MMA1 | 2 | - | 6 | 2 |
| MMA08 | MANL | - | - | 6 | 15 |
| MRQ01 | MRQ1 | 6 | - | - | 4 |
| NEJ43 | NE43 | 3 | - | - | - |
| NEJ44 | NE44 | 2 | - | 3 | 3 |
| NVY01 | NVY1 | 3 | - | 2 | - |
| NVY03 | NVY3 | 1 | - | - | - |
| NVY03[c] | NVX3 | - | - | 2 | - |
| NVY03 RM 3 | NVE3 | - | - | - | 2 |
| NVY04 | NVY4 | 2 | - | 4 | 2 |
| PLW11 | PL11 | 5 | - | - | - |
| PMG01[c] | PMX1 | 2 | - | 4 | 2 |
| PNG03 | PNG3 | - | - | - | 1 |
| PNG05 | PNG5 | 12 | 3 | 6 | 2 |
| QZN03 RM 2 | QZE3 | - | - | - | 3 |
| QZN05 | QZN5 | 2 | - | - | - |
| QZN07 | QZN7 | - | - | 2 | 2 |
| TRC02 RM 1 | TRE2 | - | - | 3 | 2 |
| ZGS02 | ZGS2 | 6 | - | - | - |

| IGS Station | DOMES Number[d] | PICMP93 | PSP94 | PICMP96 | PICMP98 |
|---|---|---|---|---|---|
| GUAM | 50501M002 | - | - | 6 | 15 |
| SHAO | 21605M002 | - | - | 6 | 12 |
| TAEJ | 23902M001 | - | 3 | 4 | 14 |
| TIDB | 50103M108 | 11 | 3 | 6 | 15 |
| USUD | 21729S007 | 5 | 3 | 6 | 15 |
| YAR1 | 50107M004 | 9 | 3 | 5 | 14 |

[a]Session lengths were 12 hours in 1993 and 24 hours in 1996 and 1998.
[b]PICMP, Philippine Islands Crustal Motion Project; PSP, Philippine Sea Plate Project.
[c]In two cases the geodetic monument was displaced between two surveys (by treasure seekers at NVY03 between 1993 and 1996 and probably by road work at PMG01 between 1990 and 1993). In these cases we give the mark a different code following the displacement.
[d]The DOMES number is a unique identifier for space-geodetic monuments, maintained by the International Earth Rotation Service (IERS).

*van*, 2001; Silcock, thesis in preparation, 2001], to enable postseismic and eventually interseismic deformation to be monitored. The 1993 measurements used dual-frequency squaring receivers (Trimble 4000SST) and multiple 12-hour measurement sessions. The Luzon network was partially resurveyed in May 1996 and May 1998 using full-wavelength dual-frequency receivers (Trimble 4000SSE and 4000SSi) with between one and six 24-hour

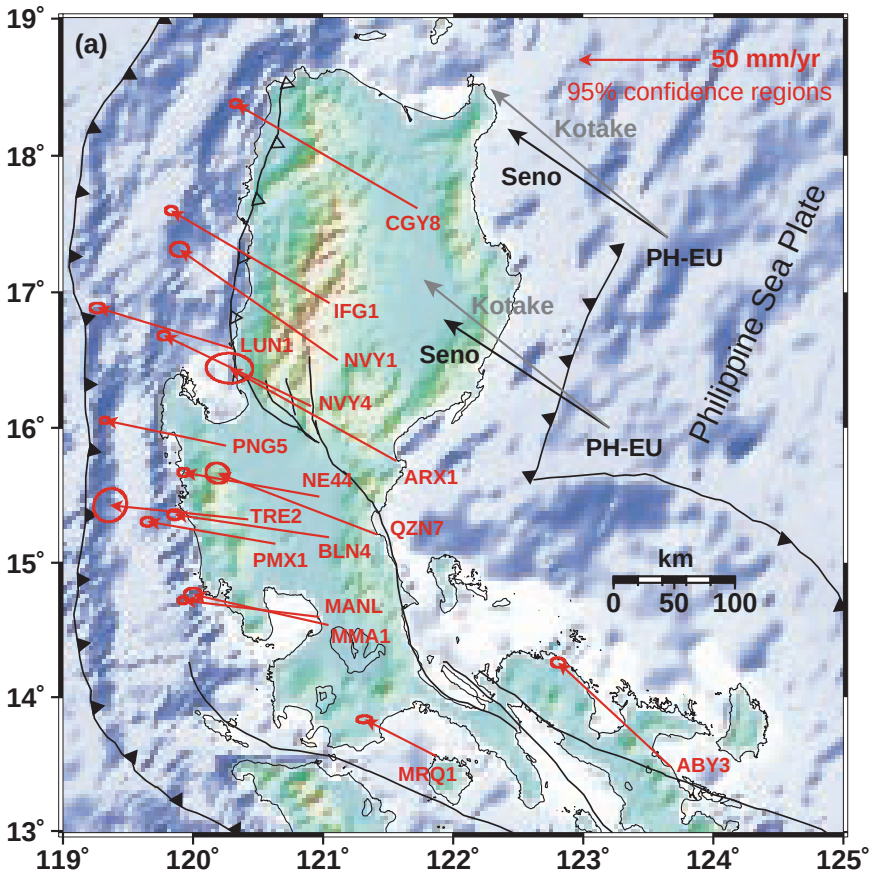


**Figure 3.** (a) Observed velocities (red arrows with 95% confidence error ellipses) of our Luzon stations relative to stable Eurasia, using the EU-ITRF96 Euler vector from Table 4. PH-EU relative plate velocities from *Seno et al.*'s [1993] model are shown in black, while those from *Kotake et al.* [1998] are in grey. (b) Observed velocities relative to PH of our stations (red arrows), *Yu et al.*'s [1999] stations (blue arrows), and *Rangin et al.*'s [1999] stations (black arrows), using the AU-ITRF96 Euler vector of Table 5 and assuming the PH-PA Euler vector of *Seno et al.* [1993] and the PA-AU Euler vector of Beavan et al. (submitted manuscript, 2001). See Table 6 for a summary of the Euler vectors used. (c) Observed velocities relative to NE Luzon assuming the rapid 5.5°/Myr rotation of Luzon relative to PH proposed by *Rangin et al.* [1999].

sessions at each station (Table 1). In addition, 3 days of 24-hour sessions were recorded at two stations in May 1994 (Table 1), which provides extra information for the velocity estimates at these stations as well as additional reference frame control.

[12] In addition to our observations, *Yu et al.* [1999] report velocities at 14 stations (one of which is in common with ours) in and near Luzon from three epochs of GPS observations taken between March 1996 and February 1998. Two of *Yu et al.*'s [1999] stations are the same two stations for which *Rangin et al.* [1999] report velocities based on 1994 and 1996 GPS measurements separated by 17 months.

### 2.2. GPS Analysis

[13] Our 1993, 1994, 1996, and 1998 data were processed using the Bernese V4.0 software [*Rothacher and Mervart*, 1996]. Our processing

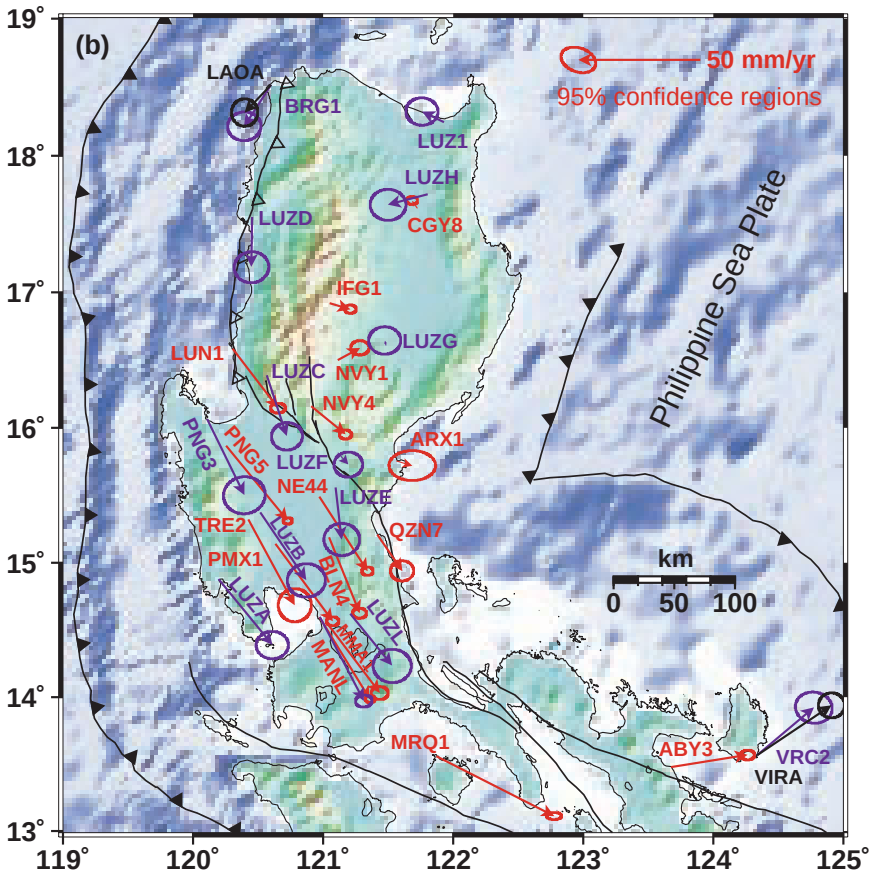


**Figure 3.** (continued)

uses standard techniques based on the double-difference phase observable, including tropospheric and ionospheric modeling, and fixing wide-lane and narrow-lane double-difference ambiguities to integers where possible. The result of each day's processing is a set of coordinate and covariance files for the stations observed that day. Further details are given by *Beavan et al.* [1999]. As usual, the error estimates output from the GPS processing package are scaled, in our case by a factor of 6, to account for unmodeled correlations between the successive 120-s GPS phase samples used in the last stage of our analysis. The factor of 6 is derived from the repeatability of daily coordinate estimates within each survey, using geodetic network adjustment software ADJCOORD [*Bibby*, 1982; *Crook*, 1992], and does not account for longer-term correlations likely to be present in the GPS data [e.g., *Zhang et al.*, 1997].

[14] We use International GPS Service (IGS) ITRF96 orbits for the 1994, 1996, and 1998 analyses and Scripps Institution of Oceanography (SIO) reprocessed ITRF93 precise orbits for 1993. We convert the original IGS orbits for the 1994 and 1996 observations to ITRF96 using global-average parameters derived by *Kouba and Mireault* [1997]; we do not use their parameters to convert SIO ITRF93 orbits to ITRF96 because we cannot be sure that the IGS and SIO realizations of ITRF93 are consistent. Regional IGS stations (Figure 2; Table 1) were added to the 1994, 1996, and 1998 processing so that the

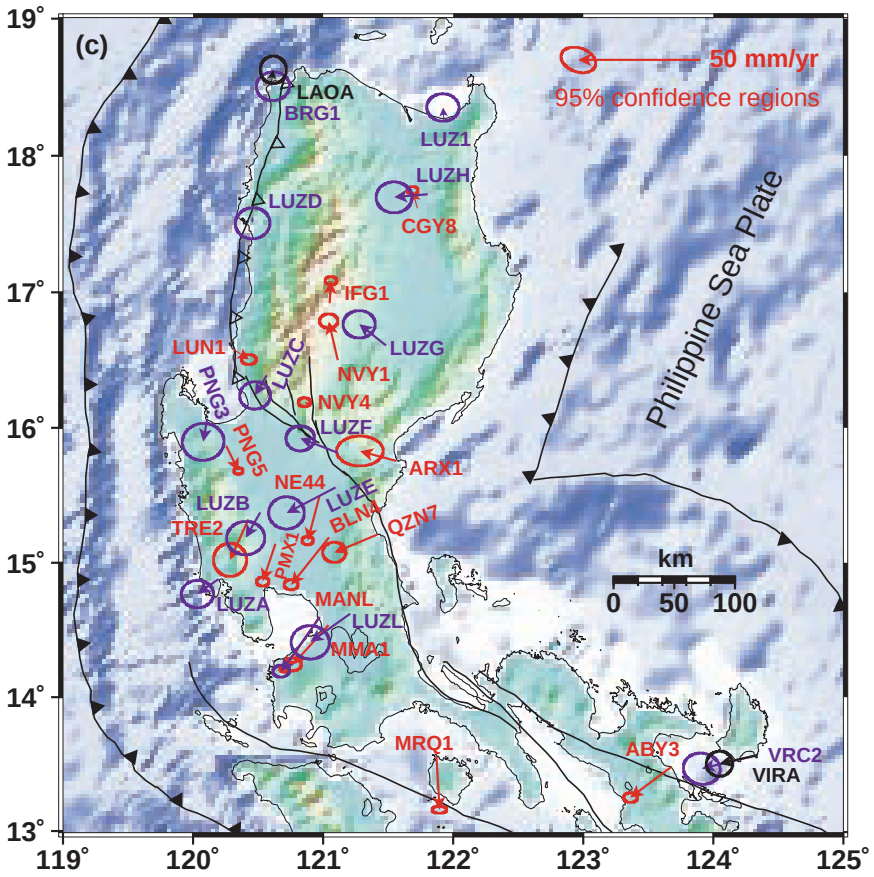


**Figure 3.** (continued)

results could be put strictly into the ITRF96 reference frame. We also attempted to use regional IGS stations TAIW, USUD, TIDB, and YAR1 for the 1993 processing, but we were unable to solve these longer baselines with sufficient accuracy to improve the reference frame definition.

### 2.3. *Velocities in ITRF96 Reference Frame*

[15] We show later that the velocities of stations in the Philippines, even those in the 1990 earthquake zone, do not change significantly between 1993–1996 and 1996–1998. Therefore we use a least squares filtering procedure with full covariance propagation to estimate the ITRF96 coordinates and velocities of all stations observed during more than one epoch (Figures 2 and 3). This procedure (1) defines the reference frame by the ITRF96 coordinates and velocities [*Boucher et al.*, 1998] of the IGS stations listed in the bottom section of Table 1, (2) calculates a seven-parameter transformation of each day's coordinate/covariance results to best fit the reference frame definition, and (3) assumes that the velocities of nonreference stations are constant (or slowly varying with a time constant of tens or hundreds of years) within the uncertainties of the daily coordinate estimates.

[16] By this procedure the stations measured only in 1993 are put strictly into the ITRF96 reference frame, even though the 1993 analysis

**Table 2.** PICMP93 Coordinates in ITRF96 Reference Frame, Epoch April 27, 1993

| Name | Latitude[a] | Longitude | Height, m | $\sigma_N$, mm | $\sigma_E$, mm | $\sigma_U$, mm |
|---|---|---|---|---|---|---|
| ABY3 | 13°28′36.03122″ | 123°40′33.32014″ | 161.753 | 9 | 10 | 19 |
| ARA1 | 15°45′25.80163″ | 121°33′47.22226″ | 47.531 | 9 | 10 | 28 |
| BLN4 | 15°11′23.95946″ | 121°2′39.55001″ | 119.531 | 9 | 9 | 23 |
| CGY8 | 17°37′2.56840″ | 121°43′35.42434″ | 82.071 | 9 | 9 | 19 |
| CTN1 | 7°0′44.44646″ | 125°5′30.85655″ | 367.214 | 23 | 42 | 45 |
| IFG1 | 16°55′14.10981″ | 121°3′5.53681″ | 1406.992 | 9 | 9 | 21 |
| ILN1 | 18°23′41.34466″ | 120°35′49.04940″ | 41.136 | 14 | 28 | 39 |
| ILO1 | 10°42′36.55341″ | 122°33′53.57592″ | 84.002 | 18 | 36 | 40 |
| LUN1 | 16°34′57.20413″ | 120°18′15.94131″ | 84.106 | 9 | 9 | 20 |
| LYT8 | 11°15′4.95009″ | 125°0′19.32413″ | 88.243 | 21 | 39 | 43 |
| MMA1 | 14°32′13.81813″ | 121°2′23.13304″ | 69.400 | 20 | 20 | 38 |
| MRQ1 | 13°33′36.03360″ | 121°52′7.98181″ | 319.041 | 14 | 31 | 38 |
| NE43 | 15°56′27.23670″ | 121°2′40.41204″ | 437.470 | 9 | 10 | 25 |
| NE44 | 15°29′29.58279″ | 120°58′10.44313″ | 100.582 | 14 | 16 | 29 |
| NVY1 | 16°30′8.20432″ | 121°6′45.50491″ | 419.297 | 11 | 12 | 26 |
| NVY3 | 16°7′59.15274″ | 120°55′48.05042″ | 979.043 | 20 | 20 | 38 |
| NVY4 | 16°9′31.58113″ | 120°54′26.86814″ | 1141.628 | 8 | 9 | 26 |
| PL11 | 9°42′27.86290″ | 118°42′51.58263″ | 55.782 | 22 | 37 | 43 |
| PMX1 | 15°8′24.80407″ | 120°37′59.56848″ | 107.131 | 14 | 16 | 31 |
| PNG5 | 15°52′3.65079″ | 120°15′13.27418″ | 139.885 | 8 | 9 | 5 |
| QZN5 | 14°39′54.06895″ | 121°36′19.15174″ | 47.657 | 12 | 13 | 30 |
| ZGS2 | 6°55′21.09511″ | 122°4′8.81300″ | 77.161 | 21 | 39 | 43 |

[a]Coordinates are obtained by propagating back to April 1993 the final coordinates and velocities from the least squares combination of the 1993-1994-1996-1998 data.

used ITRF93 orbits and no regional IGS stations were incorporated in that analysis. This is possible because (1) the 1994, 1996, and 1998 coordinates are all in the same reference frame and (2) sufficient stations were measured in each year that this reference frame can be propagated back into the 1993 data, assuming constant velocities at those stations that appear in the 1993 and at least two other data sets. Table 2 gives the ITRF96 coordinates of the stations observed in 1993, which are used by Silcock (thesis in preparation, 2001) to transform the earlier 1989–1990 single-frequency results into ITRF96. Table 3 gives the ITRF96 velocities of all stations observed in more than two surveys.

### 2.4. ITRF96 Velocities From Other Authors

[17] To obtain ITRF96 velocites from the work of *Rangin et al.* [1999], we took the ITRF96 velocities directly from the Geodyssea Web site: http://www.geologie.ens.fr/~vigny/geodyssea-itrf96-table.html. Table 1 of *Yu et al.* [1999] reports velocities in an "EU-fixed" frame which they determined by subtracting the ITRF96 velocity of station SHAO (Shanghai) (35.2 mm/yr in azimuth 112°) from all stations, then adding *Heki*'s [1996] estimate of the velocity of SHAO relative to stable Eurasia (11.1 ± 1.2 mm/yr in azimuth 112° ± 1°). This procedure for obtaining velocities relative to EU is flawed because it ignores the fact that EU is rotating with respect to ITRF96 and also assumes a flat Earth. However, the transformation information provided by *Yu et al.* [1999] allows us to convert their EU-fixed velocities back into their realization of ITRF96 by simply reversing their two velocity translations.

### 2.5. EU-Fixed and PH-Fixed Velocities

[18] The ITRF96 velocities may be transformed into a reference frame fixed to stable Eurasia by

**Table 3.** PICMP Velocities in Various Reference Frames

| | | | ITRF96 | | | | EU Fixed[a] | | PH Fixed[b] | |
|---|---|---|---|---|---|---|---|---|---|---|
| Name | Lon, deg | Lat, deg | Ve, mm/yr | Vn, mm/yr | σ Ve,[c] mm/yr | σ Vn,[c] mm/yr | Ve, mm/yr | Vn, mm/yr | Ve, mm/yr | Vn, mm/yr |
| ABY3 | 123.676 | 13.477 | −19.6 | 33.4 | 1.7 | 1.1 | −46.3 | 42.9 | 31.4 | 5.0 |
| ARX1 | 121.563 | 15.757 | −41.4 | 28.8 | 5.6 | 3.6 | −68.4 | 37.9 | 6.5 | −2.0 |
| BLN4 | 121.044 | 15.190 | −36.2 | 0.3 | 1.7 | 1.3 | −63.2 | 9.3 | 12.6 | −31.2 |
| CGY8 | 121.727 | 17.617 | −47.4 | 33.8 | 1.3 | 1.0 | −74.6 | 42.9 | −2.2 | 3.1 |
| IFG1 | 121.052 | 16.921 | −37.8 | 28.9 | 1.4 | 1.0 | −65.0 | 37.9 | 8.4 | −2.5 |
| LUN1 | 120.304 | 16.583 | −28.3 | 8.0 | 1.9 | 1.1 | −55.5 | 16.8 | 18.6 | −24.3 |
| MANL | 120.973 | 14.598 | −28.9 | −2.2 | 1.1 | 0.9 | −55.9 | 6.8 | 20.7 | −33.7 |
| MMA1 | 121.040 | 14.537 | −28.6 | 3.6 | 2.0 | 1.6 | −55.6 | 12.6 | 21.1 | −27.9 |
| MRQ1 | 121.869 | 13.560 | −2.7 | 5.9 | 1.9 | 0.9 | −29.5 | 15.1 | 48.4 | −24.6 |
| NE44 | 120.970 | 15.492 | −28.5 | 1.0 | 1.4 | 1.0 | −55.6 | 9.9 | 19.8 | −30.6 |
| NVY1 | 121.113 | 16.502 | −37.8 | 36.3 | 2.2 | 1.7 | −64.9 | 45.3 | 9.1 | 4.9 |
| NVY4 | 120.907 | 16.159 | −33.3 | 20.1 | 1.4 | 1.1 | −60.4 | 29.0 | 14.1 | −11.5 |
| PMX1 | 120.633 | 15.140 | −25.4 | 0.2 | 1.4 | 1.1 | −52.5 | 9.1 | 23.5 | −31.7 |
| PNG5 | 120.254 | 15.868 | −22.6 | 1.6 | 1.1 | 0.7 | −49.7 | 10.4 | 25.3 | −30.8 |
| QZN7 | 121.415 | 15.211 | −38.4 | 16.1 | 2.9 | 2.4 | −65.5 | 25.1 | 10.3 | −15.0 |
| TRE2 | 120.426 | 15.323 | −29.7 | −3.0 | 4.0 | 4.0 | −56.7 | 5.8 | 19.0 | −35.2 |

[a]Using EU-ITRF96 Euler vector from Tables 4 and 6.
[b]Using AU-ITRF96 Euler vector from Table 5, PA-AU Euler vector of Beavan et al. (submitted manuscript, 2001), and PH-PA Euler vector of *Seno et al.* [1993] scaled by 0.9562. See Table 6.
[c]The uncertainties are standard errors, scaled by 1.5 to attempt to account for nonwhite noise in the GPS time series.

estimating the Euler vector of Eurasia relative to ITRF96 from the ITRF96 velocity solution of the CODE Analysis Center (ftp://ftp.unibe.ch/aiub/BSWUSER/STA/ITRF96.VEL) see also *Boucher et al.*, 1998]. Using the stations in Table 4 to define stable Eurasia (very similar to the set of stations used by *Chen et al.* [2000]), we find a Euler vector 58.9°N, 95.9°W, 0.260°/Myr, with velocity residuals <2 mm/yr at this set of stations. Applying this Euler rotation to the ITRF96 velocities of Table 3 gives velocities relative to stable Eurasia, as shown in later columns of Table 3 and in Figure 3a. As a partial check on our procedure for transforming to an EU-fixed frame, we find the velocity of SHAO relative to stable Eurasia to be 6.5 mm/yr at 130° (Table 4), with estimated uncertainties of <2 mm/yr and <10°. This does not differ at the 5% significance level from the GPS estimates of 7.3 ± 2.5 mm/yr at 112° ± 9° by *Chen et al.* [2000] or 9.5 ± 1.3 mm/yr at 107° ± 7° by *Shen et al.* [2000], though it is different at this significance level from the earlier very long baseline interferometry (VLBI) estimate of 11.1 ± 1.2 mm/yr at 112° ± 1° by *Heki* [1996].

[19] Also shown in Figure 3a are the velocities of the Philippine Sea Plate relative to Eurasia predicted by two models. The model of *Seno et al.* [1993] is based on earthquake slip vectors, adjusted within error estimates to satisfy geological and tectonic boundary conditions on various plate boundary segments and assuming the NUVEL-1 relative Euler vector between Eurasia and the Pacific. In Figure 3a we have scaled the *Seno et al.* [1993] vectors by 0.9562 to attempt to account for the rescaling of NUVEL-1 to NUVEL-1A [*DeMets et al.*, 1994]. The model of *Kotake et al.* [1998] is based on a few years of GPS observations at four sites in the northern half of the Philippine Sea Plate.

[20] To transform our station velocities within Luzon into a reference frame fixed to the

**Table 4.** Euler Vector Between ITRF96 and Stable Eurasia

| Name | DOMES Number[a] | N Residual, mm/yr | E Residual, mm/yr |
|---|---|---|---|
| | *Misfits to Best Fit Euler Vector*[b] | | |
| BOR1 | 12205M002 | −0.5 | −0.7 |
| BRUS | 13101M004 | −0.3 | 0.4 |
| HERS | 13212M007 | 0.8 | 1.3 |
| IRKT | 12313M001 | −1.2 | −1.4 |
| KIT3 | 12334M001 | −0.3 | 1.3 |
| KOSG | 13504M003 | 0.4 | −0.2 |
| METS | 10503S011 | −1.4 | 0.3 |
| NYAL | 10317M001 | 0.3 | 1.5 |
| ONSA | 10402M004 | −1.3 | −0.3 |
| POL2 | 12348M001 | 2.1 | 0.9 |
| POTS | 14106M003 | −0.2 | 0.8 |
| TROM | 10302M003 | 1.8 | −1.8 |
| VILL | 13406M001 | −0.3 | −1.0 |
| WTZR | 14201M010 | −0.9 | 0.4 |
| RMS misfit | | 1.0 | 1.2 |
| | *Velocities Relative to Stable Eurasia* | | |
| SHAO | 21605M002 | −4.1 | 5.0 |
| TAEJ | 23902M001 | −4.9 | 3.3 |
| TAIW | 23601M001 | −1.9 | 8.9 |
| WUHN | 21602M001 | −0.5 | 8.5 |

[a]The DOMES number is a unique identifier for space-geodetic monuments, maintained by the IERS.
[b]Our calculated Euler vector between ITRF96 and stable Eurasia is 58.9°N, 95.9°W, 0.260°/Myr.

Philippine Sea Plate (PH), we could use our EU-fixed velocities and the EU-PH Euler pole of *Seno et al.* [1993]. However, for several reasons we believe it is preferable to transform from ITRF96 to PH-fixed via the Australian (AU) and Pacific (PA) Plates, rather than via EU. The first reason is that determinations of AU-ITRF Euler vectors by different workers are much more stable than determinations of EU-ITRF vectors [e.g., *Larson et al.*, 1997; *Tregoning et al.*, 1998; P. Tregoning, Plate kinematics in the western Pacific derived from geodetic observations, submitted to *Journal of Geophysical Research*, 2001 (hereinafter referred to as Tregoning, submitted manuscript, 2001), Table 1] (Table 5). This is probably because EU is not rigid, and different workers define "stable" Eurasia by different sets of stations, whereas *Tregoning et al.* [1998] and Tregoning (submitted manuscript, 2001) demonstrate that AU is rigid to within ~1 mm/yr. The second reason is that *Seno et al.*'s [1993] strongest result is the Euler vector between PA and PH; their EU-PH vector depends on the accuracy of the NUVEL-1 EU-PA Euler vector. The third reason is that the PA-AU Euler vector is now well known. The PA-AU Euler vectors of *Tregoning et al.* [1998] and Tregoning (submitted manuscript, 2001) have been updated with additional data by J. Beavan et al. (Motion and stability of the Pacific Plate, submitted to *Journal of Geophysical Research*, 2001) (hereinafter referred to as Beavan et al., submitted manuscript, 2001), and the two recent estimates give very similar velocities (differing by <2 mm/yr) in Luzon when used in our transformation from ITRF96 to PH-fixed. The AU-ITRF96 Euler vector we use is derived from the ITRF96 velocities of the four AU stations that have the most reliable velocities in the ITRF96 definition and is in very good agreement with independently derived Euler vectors (Table 5). All Euler vectors we use in the transformation are summarized in Table 6,

**Table 5.** Euler Vector Between ITRF96 and Australia

| Name | DOMES Number[a] | N residual, mm/yr | E residual, mm/yr |
|---|---|---|---|
| | *Misfits to best fit Euler vector*[b] | | |
| TIDB | 50103M108 | 0.21 | 0.18 |
| YAR1 | 50107M004 | 0.17 | 0.18 |
| HOB2 | 50116M004 | 0.31 | 0.29 |
| PERT | 50133M001 | 0.07 | 0.11 |
| RMS misfit | | 0.24 | 0.23 |

[a]The DOMES number is a unique identifier for space-geodetic monuments, maintained by the IERS.
[b]Our calculated Euler vector between ITRF96 and AU is 33.7°N, 42.3°E, 0.650°/Myr. For comparison, *Kreemer et al.* [2000] find 34.4°N, 43.5°E, 0.64°/Myr between ITRF96 and AU, while *Tregoning et al.* [1998] find 31.6°N, 41.3°E, 0.62°/Myr between ITRF94 and AU, and Beavan et al. (submitted manuscript, 2001) find 34.63°N, 37.08°E, 0.615°/Myr between ITRF97 and AU.

and the resulting PH-fixed velocities are shown as red arrows in Figure 3b and are listed in the last two columns of Table 3.

[21] Using the EU-PH Euler vector of *Kotake et al.* [1998] instead of that of *Seno et al.* [1993] to transform from the velocities of Figure 3a to PH-fixed adds a SSE directed velocity of ~18 mm/yr to all the velocity estimates in Figure 3b. This implies geologically unlikely left-lateral motion of this magnitude between the northeast coast of Luzon and the rigid Philippine Sea Plate.

[22] Also shown in Figure 3b are the 14 GPS velocities determined by *Yu et al.* [1999] (blue arrows) and the two by *Rangin et al.* [1999] (black arrows), which we have transformed from their realizations of ITRF96 to PH-fixed using the same set of Euler vectors (Table 6) we used for our velocities. Two of the sites used by *Yu et al.* [1999], BRG1 and VRC2, are the same physical points as sites LAOA and VIRA of *Rangin et al.* [1999] but with data collected independently by the two groups.

[23] The velocities determined by the different groups look reasonably consistent in Figure 3b, though there is a hint of a counterclockwise rotation of *Yu et al.*'s [1999] velocities relative to ours, which we will quantify later. The velocities at the only site common to *Yu et al.*'s [1999] network and ours (MANL) agree closely. The velocities estimated by *Yu et al.* [1999] and

**Table 6.** Euler Vectors Used in This Paper[a]

| Plate Pair | Source | Latitude, °N | Longitude, °E | Rate, °/Myr |
|---|---|---|---|---|
| EU-ITRF96 | this paper | 58.9 | −95.9 | 0.260 |
| AU-ITRF96 | this paper | 33.7 | 42.3 | 0.650 |
| PA-AU | Beavan et al. (submitted manuscript, 2001) | −61.65 | 185.18 | 1.088 |
| PH-PA[b] | *Seno et al.* [1993] | 1.24 | 134.19 | −0.956 |
| PH-EU[b] | *Seno et al.* [1993] | 48.23 | 156.97 | −1.037 |
| PH-EU | *Kotake et al.* [1998] | 41.55 | 152.46 | −1.50 |

[a]The Euler vectors give the counterclockwise rotation of the first-named plate relative to the second, as viewed looking down onto the Earth's surface.
[b]Rotation rates scaled by 0.9562 from the values of *Seno et al.* [1993] to attempt to account for timescale change between NUVEL-1 and NUVEL-1A.

*Rangin et al.* [1999] for their two common sites are equivalent at the 5% significance level.

## 3. Tectonics and Rotation of Luzon

[24] *Rangin et al.* [1999] use the velocities at their two stations LAOA and VIRA to infer that Luzon comprises a relatively undeformed block rotating counterclockwise relative to PH at ~5.5°/Myr about a point in northern Luzon. We describe the sense of rotation as viewed from a vantage point looking down on the Earth. This inference comes from the good fit of this Euler vector to these two velocities, after they first make a correction of ~25 mm/yr to the velocity of VIRA to account for interseismic elastic deformation under the assumption that the Philippine Trench is presently fully locked. *Rangin et al.* [1999] acknowledge that the results of *Yu et al.* [1999] imply ~20 mm/yr present-day motion along the Philippine fault system in central Luzon but claim that this does not change the main conclusions of *Rangin et al.* [1999].

[25] We believe that the deformation field in Luzon is much better characterized as predominantly strike-slip motion along the Philippine fault system. There is no evidence for rapid counterclockwise rotation of Luzon relative to PH, though we show later that there may be a much slower rotation of 1°–2°/Myr. This can be seen to some extent in Figure 3b, where the rapid change in fault-parallel velocity across the Philippine fault system is consistent with strike-slip motion; a rotation would be indicated by a uniformly increasing velocity rather than the observed rapid change across the fault. The predominance of strike-slip motion is even clearer in the cross-section plots discussed below (Figures 4 and 6), and has also been found by *Thibault* [1999] in her combined analysis of the 1996–1998 campaigns with those of *Yu et al.* [1999]. Little or no present-day rotation of Luzon relative to PH is supported by paleomagnetic observations. Though *Rangin et al.* [1999] quote *McCabe et al.* [1982] in support of rapid rotation, a more appropriate reference is *Fuller et al.* [1983]. *Fuller et al.* [1983] show convincingly that northern Luzon has not been rotating (or possibly has been rotating slightly clockwise) for the past 5 Myr, even though there was pronounced counterclockwise rotation throughout the Miocene. This lack of rotation is relative to a geographic reference frame, which is approximately aligned with the NUVEL-1A no-net-rotation (NNR-A) reference frame and therefore with ITRF reference frames (which are designed to be aligned with NNR-A). Since PH is rotating clockwise at ~0.9°/Myr with respect to these frames, we infer on this basis a small counterclockwise rotation of Luzon relative to PH, but at a rate <20% of the 5.5°/Myr rotation envisaged by *Rangin et al.* [1999].

[26] We show in Figure 3c the velocity field within Luzon relative to *Rangin et al.*'s [1999] Luzon reference frame. Under their hypothesis all stations should show zero velocity unless affected by elastic strain accumulation. The velocity of LAOA is small, and the velocity of VIRA could be construed as resulting from elastic deformation, as assumed by *Rangin et al.* [1999]. However, apart from these stations and a couple of others in northernmost Luzon, it is clear that the deformation pattern is not consistent with rapid rotation of Luzon relative to PH. The value of $\sqrt{\chi^2}_R$ for the difference between the velocity field of Figure 3c and zero is 10.2, compared to values of ~2 that we find in later modeling.

## 4. Modeling of Deformation Following the 1990 Earthquake

### 4.1. Evolution of Deformation

[27] To examine the evolution of deformation following the 1990 earthquake, we first analyze the 1993, 1996, and 1998 surveys together,

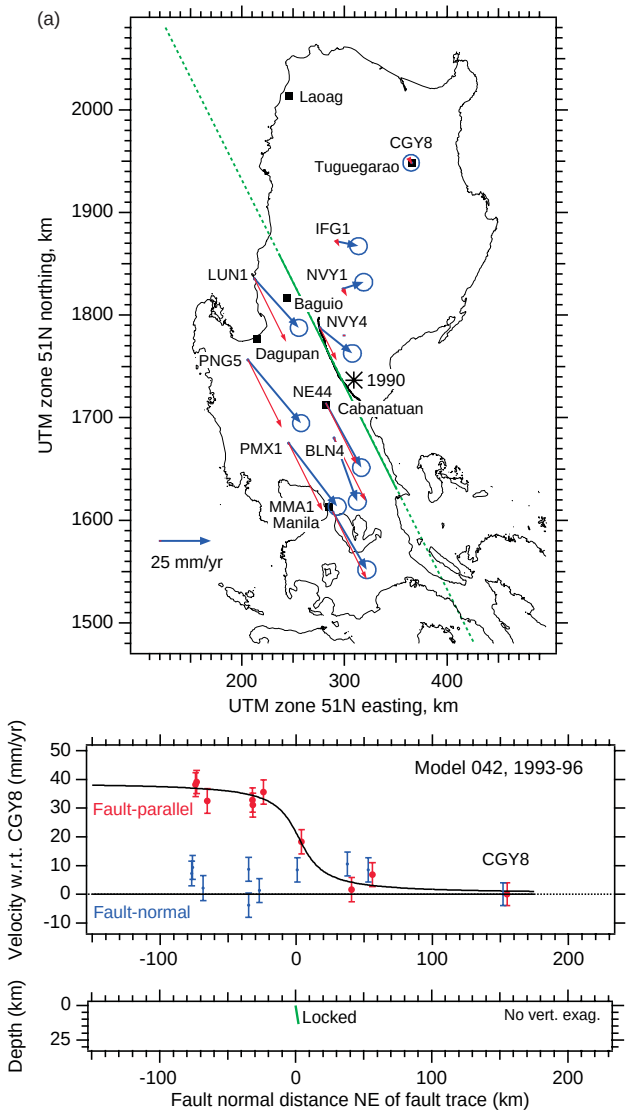


**Figure 4.** Observed velocities (thick blue arrows with 95% confidence error ellipses), fault-normal profiles, and locked-fault models (a) from our 1993–1996 GPS observations, (b) from our 1996–1998 observations (both with station CGY8 held fixed), and (c) as reported by *Yu et al.* [1999] but translated by transforming into a reference frame oriented with ITRF96, then holding LUZ1 fixed. The slight nonzero velocities of the "fixed" stations result from small translations estimated during the dislocation model inversion. The positive bias in the fault-normal velocities in Figure 4a is probably an artifact of holding station CGY8 nearly fixed. In Figure 4b the label for MMA1 is omitted for clarity. Also shown are the velocities (thin red arrows) predicted by elastic half-space models in which steady slip is occurring below locking depth $D$ on a long strike-slip fault. In the profiles the observed fault-parallel velocities are shown by large red dots with 1σ error bars. The fault normal velocities are shown as small blue dots with 1σ errors. The bottom panel shows the locked zone up dip of the steadily slipping fault whose parameters we have modeled. The surface trace of the viscoelastic coupling model is shown on the maps as a solid green line and by a dashed green line where it is unconstrained by our surface velocity data. Distances in the profiles are along the azimuth determined in the inversion projected onto a line through the point on the 1990 rupture trace closest to the 1990 epicenter. The mapped surface trace of the 1990 earthquake is shown by the curved black line.

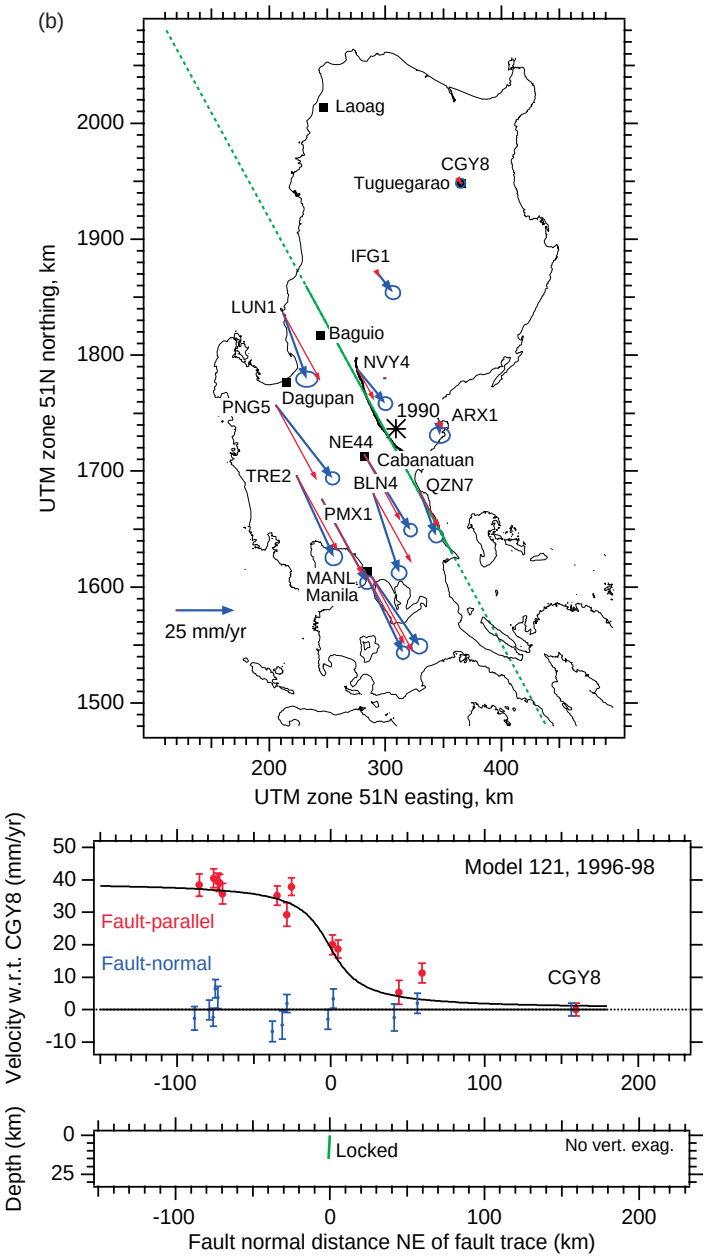


**Figure 4.** (continued)

solving only for stations that are observed in all three surveys and are well away from the 1990 fault trace. This allows us to estimate the rotation of the 1993 reference frame relative to the ITRF96-oriented reference frame used for the 1996 and 1998 data. We find that none of the transformation parameters are statistically significant, so we assume for subsequent calculations that the 1993 data are in the same reference frame as the later data. We then use ADJCOORD [*Bibby*, 1982; *Crook*, 1992] to solve simultaneously for the coordinates and

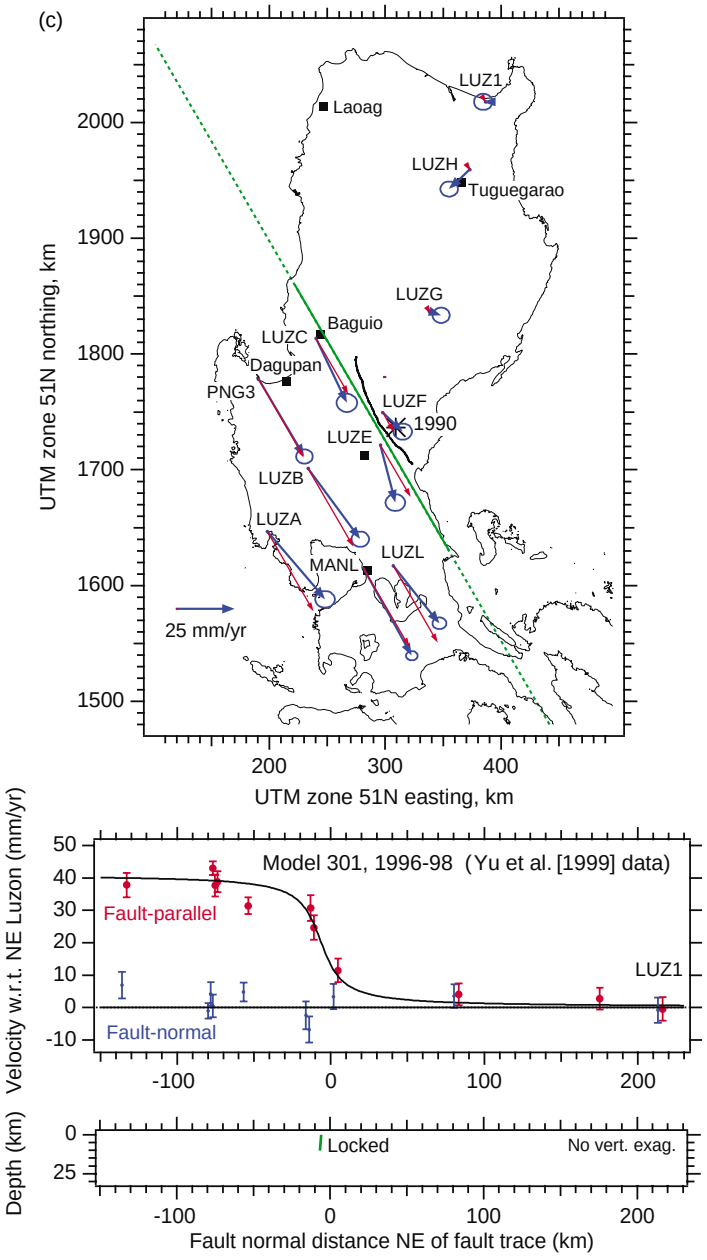


**Figure 4.** (continued)

velocities of all our Luzon stations observed in (1) the 1993–1996 interval and (2) the 1996–1998 interval (Figures 4a and 4b). We retain full covariance information throughout the inversion procedure and fix one station (CGY8) in northeastern Luzon as a minimal constraint.

[28] We then project the 1993–1996 and 1996–1998 horizontal velocity solutions onto a planar

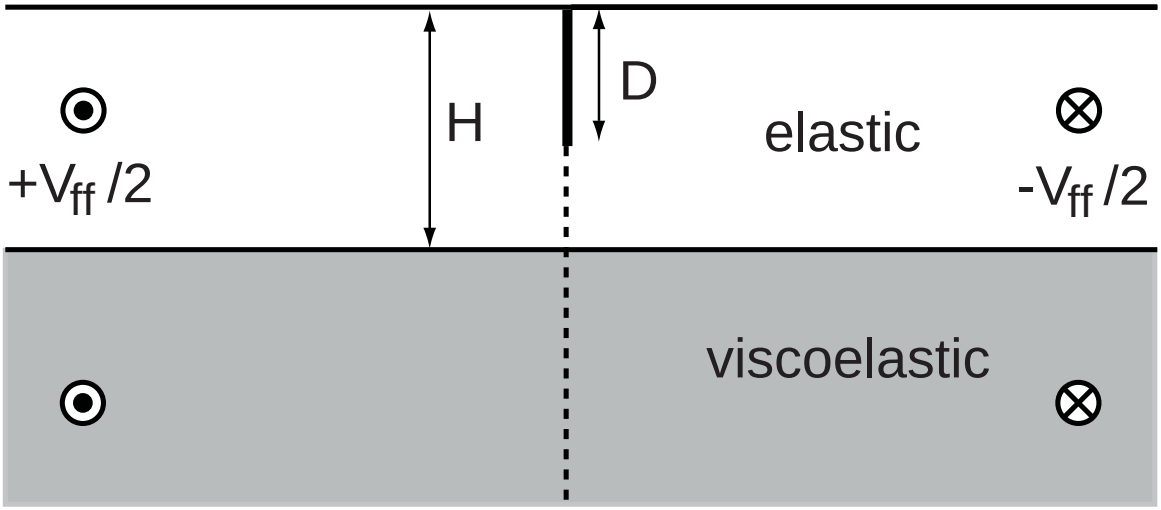


**Figure 5.** Schematic of viscoelastic model with an elastic layer overlying a viscoelastic half-space. A far-field velocity of $V_{ff}$ is applied. The elastic model is similar except that there is no viscoelastic layer ($H$ is infinite), and the far-field velocity is applied along the fault below its locking depth (i.e., along the dotted line).

coordinate system (UTM zone 51N) in preparation for elastic half-space dislocation modeling. The reference frame of the solutions shown in Figures 4a and 4b is oriented with ITRF96, but with a translation applied in the planar coordinate system to make the velocity of station CGY8 zero.

[29] We analyze *Yu et al.*'s [1999] velocity results similarly, first transforming them to the ITRF96 frame as described earlier, and then applying a translation in the planar coordinate system to set the velocity of their northernmost station (LUZ1) to zero (Figure 4c).

### 4.2. Reference Frame for Models

[30] In order to discriminate between a reference frame rotation and the far-field part of the velocity field due to slip at depth on a strike-slip fault plane, it is necessary to have data from at least two, and preferably more, distant stations on one side of the fault in order to set the reference frame relative to the fault. If the fault azimuth is known and if the style of deformation (e.g., pure strike-slip) is assumed, then an "outer coordinate" or "extrinsic" solution that minimizes root mean square (rms) velocities normal to the fault azimuth can be used to set the reference frame without the need for the distant stations [*Prescott*, 1981]. In the Luzon case we do not have well-distributed distant stations on either side of the fault, so to set the reference frame, either we can assume an azimuth for the fault and use an extrinsic solution or we can make some other assumption. For our modeling we initially leave the velocities as they are, in a frame rotating with ITRF96, and solve for the azimuth of the model fault. One justification for this is the point discussed in section 3: that paleomagnetic evidence suggests that Luzon is not presently rotating significantly relative to a geographic reference frame, nor therefore to an ITRF reference frame.

### 4.3. Elastic Modeling

[31] Surface deformation following a major strike-slip earthquake can be treated by either a "deep slip" model or a viscoelastic relaxation model (Figure 5). We first model our 1993–

1996 and 1996–1998 velocities (Figures 4a and 4b) using the dislocation method originally described by *Savage and Burford* [1970, 1973; see also *Chinnery*, 1961; *Okada*, 1985; *Cohen*, 1999]. We apply the same model to the 1996–1998 data presented by *Yu et al.* [1999] (Figure 4c). Rather than a forward model, we formally invert the surface velocity data using a nonlinear least squares inversion [*Dennis et al.*, 1981a, 1981b; *Darby and Beavan*, 2001]. We include a horizontal translation of the reference frame in the dislocation modeling so that the inversion is not constrained by any fixed station assumptions, and we retain the full variance-covariance matrix of the data in the inversion. We then discuss whether the parameters of the fault slip model are reasonable, and we also examine a range of viscoelastic relaxation models, using a mixture of forward modeling and inversion, to see if these provide an equivalent or better fit to the observed velocities.

[32] The surface velocity data have a fairly sparse spatial distribution (Figure 4), so we are not able to solve for all parameters, even of a single fault model. We therefore assume a single, long, strike-slip fault slipping at a steady rate $V_{ff}$ everywhere below the locking depth $D$. We assume a single, planar fault despite the facts that the Philippine Fault splits into several splays in central Luzon [*Allen*, 1962; *Philippine Bureau of Mines*, 1963; *Barrier et al.*, 1991] and that the surface trace of the 1990 rupture is substantially curved. The long model fault is used for simplicity and is an adequate assumption with which to estimate slip rate and to test the velocity data for changes in slip rate with time. However, it is only a first approximation, and we do not believe the strike-slip zone goes offshore as in the model; this part of the model is insensitive to the available data. The fit of the resulting models to the observed data gives reasonable support to these assumptions, except for two stations in northwestern Luzon reported by *Yu et al.* [1999]. These two stations, BRG1 and LUZD (Figure 3b), are west of the Cordillera Central and appear to be affected by convergence and strike-slip deformation across this range. We therefore omit their velocities from the elastic modeling. We expect that much of the Philippine Fault motion is transferred from the ~150° oriented fault system to a north-south oblique convergence zone including the Cordillera Central, as suggested by the geology [*Bureau of Mines and Geosciences*, 1982; *Barrier et al.*, 1991], but there are presently insufficient geodetic data to test this properly.

[33] We invert the velocity data of Figures 4a–4c using the procedure described above to solve for the slip rate, the locking depth, and the strike of the fault, initially assuming 90° dip and 0° rake (based on the slip parameters for the 1990 earthquake found by *Silcock and Beavan* [2001]), but relaxing the dip assumption in some models. We initially constrain the projection of the fault plane to cut the surface at the 1990 fault trace near the 1990 epicenter, but also relax this assumption in some models. Since we are assuming a very long model fault with pure left-lateral slip, varying the dip and varying the horizontal position of the fault are equivalent operations. This is because the surface deformation is sensitive only to the position of the screw dislocation located at the depth of transition between locked and slipping behavior.

[34] For our 1993–1996 and 1996–1998 intervals we assign an uncertainty to the north and east velocity components of station CGY8, which was fixed in the ADJCOORD analysis, and adjust the remainder of the covariance matrix appropriately. We used an uncertainty of 4 mm/yr for the 1993–1996 interval and 2 mm/yr for the 1996–1998 interval. For *Yu et al.*'s [1999] velocities there is no fixed station

**Table 7.** Elastic Dislocation Model Results for Postseismic/Interseismic Slip on the Philippine Fault System[a]

| Time Interval | $V_{ff}$, mm/yr | $D$, km | Strike, deg | Dip, deg | $\sqrt{\chi^2_R}$ |
|---|---|---|---|---|---|
| 1993–1996b[a] | 39.1 ± 8.3 | 14 ± 14 | 153 ± 6 | 98 ± 26 | 2.56 |
| 1996–1998[b] | 39.4 ± 5.4 | 15 ± 10 | 151 ± 2 | 86 ± 12 | 1.82 |
| 1996–1998[c] | 41.0 ± 4.5 | 10 ± 6 | 150 ± 3 | 85 fixed | 1.97 |
| 1996–1998[d] | 42.0 ± 3.8 | 15 ± 5 | 150 fixed | 77 ± 10 | 1.91 |

[a]The formal 1s error estimates have been scaled by $\sqrt{\chi^2_R}$, where $\chi^2_R$ is the reduced $\chi^2$, or $\chi^2$ divided by the number of degrees of freedom.
[b]Using PICMP velocity field (this paper).
[c]Using velocity field from *Yu et al.* [1999].
[d]Using velocity field from combination of PICMP and *Yu et al.* [1999] results.

in Luzon, so we use their error estimates directly, assuming all interstation correlations to be zero.

[35] The results of the inversions are given in Table 7 and Figure 4. Slip rates are determined reasonably well, at ~40 ± 5 mm/yr, because we have sufficient stations in the far field of the model fault. The strike is close to 151° in all three cases, and the dip cannot be statistically distinguished from vertical. The locking depth is determined poorly in both our 1993–1996 and 1996–1998 intervals because there are too few near-field stations to accurately describe the shape of the deformation field within 20 km of the fault. The depth determination from *Yu et al.*'s [1999] data is more precise owing to their better distribution of stations in the near field. The apparent slip rate and locking depth are each statistically indistinguishable between the 1993–1996 and 1996–1998 intervals, but given the size of the standard errors, the data allow the possibility of a slip rate change of at least 10%.

[36] We have little constraint on the apparent locking depths in the individual inversions, though they are likely to be in the range 10–15 km. For the 1996–1998 interval we take advantage of the two independent data sets and invert our 1996–1998 velocities jointly with those of *Yu et al.* [1999]. Because these are in different realizations of the ITRF96 reference frame, we take the outer coordinate solution approach [*Prescott*, 1981] in order to place both data sets in the same frame. For each data set we allow a rotation and a translation (but not a scale change) of the velocity field such that the sum of squared velocity components in direction 60°, normal to the assumed fault direction, is minimized. The resulting joint inversion (Table 7, Figure 4c) gives more precise estimates of both slip rate and locking depth, because the two data sets complement each other in terms of the distribution of stations normal to the fault. The square roots of the reduced $\chi^2$ (goodness of fit) statistics for the models are ~2. This implies either that the model is poor or that the uncertainties in the velocity observations are underestimated. Both factors probably contribute, with a factor of 1.5–2 underestimate of the uncertainties being likely as a result of the assumption of a white-noise correlation structure for the time series of GPS daily coordinate estimates [e.g., *Zhang et al.*, 1997]. The fault parameters we find (Table 7, last row) are close to those obtained by *Thibault* [1999], based on a combined analysis of the 1996–1998 campaign data and the data analyzed by *Yu et al.* [1999]. Using a trial-and-error forward modeling procedure for a single strike-slip Philippine Fault, she obtained a strike of 145°, a slip rate of 40

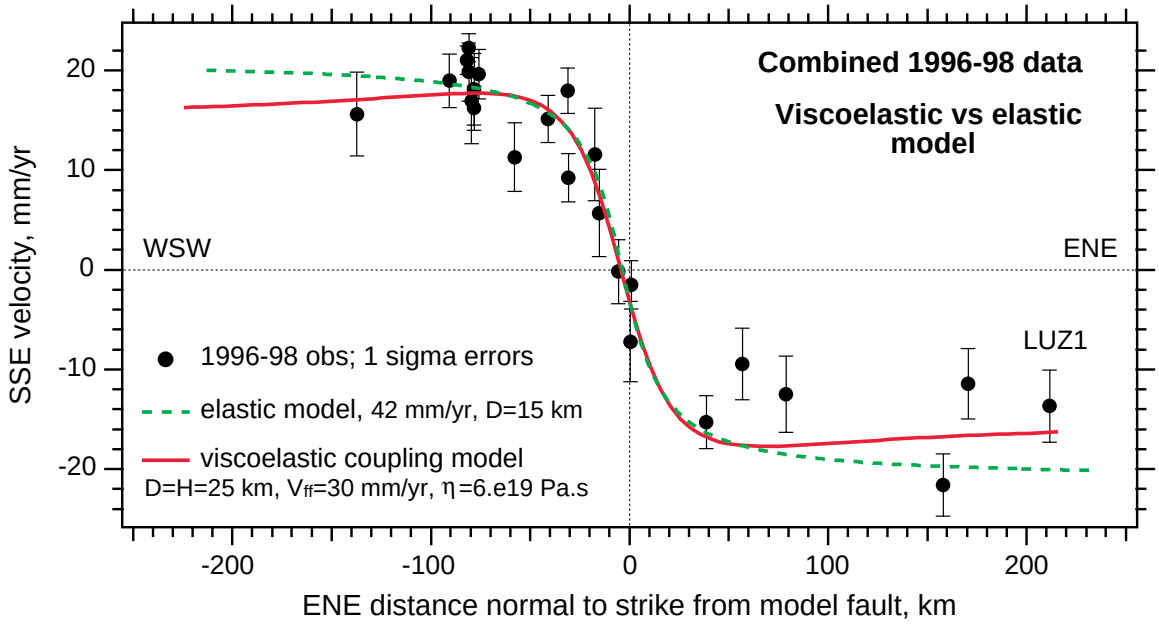


**Figure 6.** Fault-normal velocity profile obtained by combining our 1996–1998 velocities with those of *Yu et al.* [1999] (Figures 4b and 4c). Reference frames for each are chosen by allowing a rotation and translation of each data set and minimizing the RMS velocity components normal to the 150° azimuth model fault. Also shown are the best elastic half-space model (obtained by formal inversion) and one viscoelastic forward model. The parameters of the latter model are rigidity $\mu = 3 \times 10^{10}$ Pa, viscosity $\eta = 6 \times 10^{19}$ Pa s, repeat time $T = 300$ years, elastic thickness $H = 25$ km, locking depth $D = 25$ km, and long-term slip rate $V_{ff} = 30$ mm/yr.

mm/yr, a dip of 70° east, and a locking depth of 20 km.

[37] Our estimated long-term slip rate from the elastic model is 42 ± 4 mm/yr. Assuming that 5–6 m slip events are typical, this implies a recurrence time of ~120–150 years. The last event on this section of the Philippine fault system was probably in 1645, implying that the most recent interevent interval has been at least 345 years. Also, *Daligdig*'s [1997] geological and paleoseismological estimates of slip rate are generally between 15 and 20 mm/yr, and his estimated recurrence interval is 300–400 years though based on only two dated intervals. The most likely interpretation of these facts is that the long-term slip rate is overestimated by the elastic model of the 1993–1998 data. Otherwise, events with displacements much greater than 6 m must be common in this part of the Philippine fault system, or the 300–400 year intervals between the three most recent earthquakes have both been unusually long.

[38] Our estimated locking depth is 15 ± 4 km with a deeper locking depth failing to well fit the steepness of the observed velocity profile between about −20 km and +10 km (Figures 4c and 6). The earthquake hypocenter is at 25 km depth, our best geodetic estimate of the depth of coseismic rupture is ~20 km along the central part of the rupture [*Silcock and Beavan*, 2001], and the best seismological estimate is 20 km [*Yoshida and Abe*, 1992]. This suggests that the 15 km locking depth of the elastic model may be an underestimate compared to our expectations, though given the uncertainty estimates, this is not a strong conclusion.

[39] One way to explain both the apparently too fast velocity and the possibly too shallow locking depth is that we are detecting significant viscoelastic effects. These effects are accelerating the surface deformation in the years following the 1990 quake, thus biasing high the far-field velocity derived from the elastic model. They are also concentrating deformation closer to the fault than in the elastic case, perhaps biasing low the locking depth interpreted from the elastic model.

### 4.4. Postseismic Displacements Following Major Strike-Slip Earthquakes

[40] Following a major earthquake that breaks most or all the way through the elastic lithosphere ("schizosphere" in the nomenclature of *Scholz* [1990]), accelerated postseismic deformation is often observed in the near field of the fault [*Nur and Mavko*, 1974]. This has generally been interpreted as being due either to accelerated slip on a downdip extension of the coseismic fault or to flow in the ductile part of the lower lithosphere or asthenosphere as a result of stress transfer at the time of coseismic rupture (see *Cohen* [1999] for a recent review). Even if the true explanation for such deformation is viscoelastic deformation of the lower lithosphere, the resulting surface deformation for a long, vertical, strike-slip fault can always be modeled by a plausible slip distribution on a downdip extension of the fault [*Savage*, 1990], so that distinguishing between these two models requires additional information.

[41] In *Savage and Prescott*'s [1978] viscoelastic coupling model of the earthquake cycle an elastic layer of thickness $H$ overlies a Maxwell linear viscoelastic half-space (Figure 5). A long strike-slip fault extends to depth $D$ in the elastic layer, and earthquakes occur on the fault at even intervals, $T$. Between earthquakes, the fault is locked at depths shallower than $D$, and it slips below $D$ in response to an applied far-field velocity $V_{ff}$. At the time of an earthquake there is coseismic slip shallower than depth $D$, and this instantaneously transfers stress into the viscoelastic layer, which responds with accelerated deformation. In the original formulation of the model the fault in the elastic material between depths $D$ and $H$ is assumed to slip steadily at velocity $V_{ff}$. With improved understanding of Earth rheology this has been thought unrealistic, and the model has recently been used in the special case $D = H$ [e.g., *Savage and Lisowski*, 1998; *Dixon et al.*, 2000].

[42] In this and other similar models [e.g., *Li and Rice*, 1987] the magnitude and the temporal and spatial distribution of surface postseismic deformation depends on several factors. Most important are the fraction of the thickness of the elastic lithosphere that is broken coseismically, and the Maxwell time, which is the ratio of viscosity to shear modulus, $\eta/\mu$, in the ductile lower lithosphere. In general, viscoelastic effects become less pronounced when the Maxwell time is longer than ~50% of the earthquake recurrence interval or when the locking depth is much less than the thickness of the elastic layer. When viscoelastic effects are important, their tendency is to increase deformation rates in the early part of the earthquake cycle (i.e., soon after a major earthquake) and to concentrate the early deformation closer to the coseismic rupture than in the elastic case [*Savage and Prescott*, 1978; *Thatcher*, 1983; *Li and Rice*, 1987].

[43] The *Savage and Prescott* [1978] model is two dimensional, implying that the full length of the fault breaks in each earthquake. Applying this to a realistic situation, we are assuming that the fault breaks all the way through the geodetic network either in a single earthquake or in a series of earthquakes separated by much less than time $T$. The 1990 Luzon quake does not satisfy this assumption very well, as it

breaks through only ~2/3 of the along-strike dimension of the geodetic network, and adjacent parts of the fault have not broken in recent times. With these provisos we apply the model, both in its original form and in the $D = H$ version, to the Luzon data.

[44] To reduce the effects of these assumptions, we also apply a different type of model that calculates the viscoelastic response to the actual fault rupture in the 1990 earthquake using a spherically stratified Earth model with a mixture of elastic and viscoelastic layering [*Pollitz*, 1992]. This model calculates the viscoelastic effects for a single earthquake, rather than modeling the whole earthquake cycle, as done by *Savage and Prescott* [1978]. In using the model we make the assumption that viscoelastic effects due to prior earthquakes have completely died away by 1990. Also, in order to match the observed displacement data we must include a model of steady state strain accumulation as well as the postseismic model. For this we use the elastic model described in section 4.3. We have formulated our model to also estimate the rotation rate of Luzon relative to PH in order to provide a more specific test of the rapid rotation rate inferred by *Rangin et al.* [1999] and discussed earlier in section 3.

[45] From our 1993–1996 and 1996–1998 observations and *Yu et al.*'s [1999] results, we have two epochs of displacement data, from ~2.75 to ~5.75 years and ~5.75 to ~7.75 years after the earthquake. In these data we expect to see deformation related to the long-term slip rate (or far-field velocity) on the Philippine Fault in Luzon as well as possible postseismic effects.

[46] In the viscoelastic models we expect to detect changes in displacement rate between these two intervals only if the Maxwell time is particularly short (i.e., low viscosity). However, we may detect velocities higher than the long-term rate, particularly in the near field of the earthquake, if the Maxwell time is less than ~50% of the average earthquake recurrence interval.

[47] Very short-term postseismic effects, on the order of days to a few years, are sometimes observed following large earthquakes, and these are generally attributed to slip on an extension of the coseismic rupture surface or on some other nearby slip surface. Recent examples are the 1992 Landers earthquake [*Shen et al.*, 1994; *Savage and Svarc*, 1997] and the 1999 Izmit earthquake [*Reilinger et al.*, 2000]. Such effects are undetectable in our data because accurate postseismic observations did not start until nearly 3 years after the earthquake.

### 4.5. Viscoelastic Modeling Results

#### 4.5.1. Savage and Prescott model: Original formulation

[48] We show in Figures 6 and 7 and in Table 8 a variety of viscoelastic coupling models that fit the velocity data as well as or better than the elastic model. We perform a grid search for acceptable solutions, varying $D$ from 8 to 30 km, $H$ from 25 to 60 km, $\eta$ from 0.3 to 100 $\times$ $10^{19}$ Pa s, and $V_{ff}$ from 7.5 to 50 mm/yr. We deem acceptable solutions to be those for which the reduced $\chi^2$ of the fit is smaller than the reduced $\chi^2$ for the elastic solution and for which the difference between the modeled 1993–1996 and 1996–1998 velocity fields does not exceed 10% in the distance range 50–100 km from the model fault. In these examples we fix the recurrence interval to 300 years, close to *Daligdig*'s [1997] best estimate. There is a trade-off between $\eta$ and $V_{ff}$, with long-term velocity as low as 10 mm/yr fitting the data for viscosities of 0.6–0.8 $\times$ $10^{19}$ Pa s (Figure 7). These are the minimum $V_{ff}$ and $\eta$ that do not violate the condition of

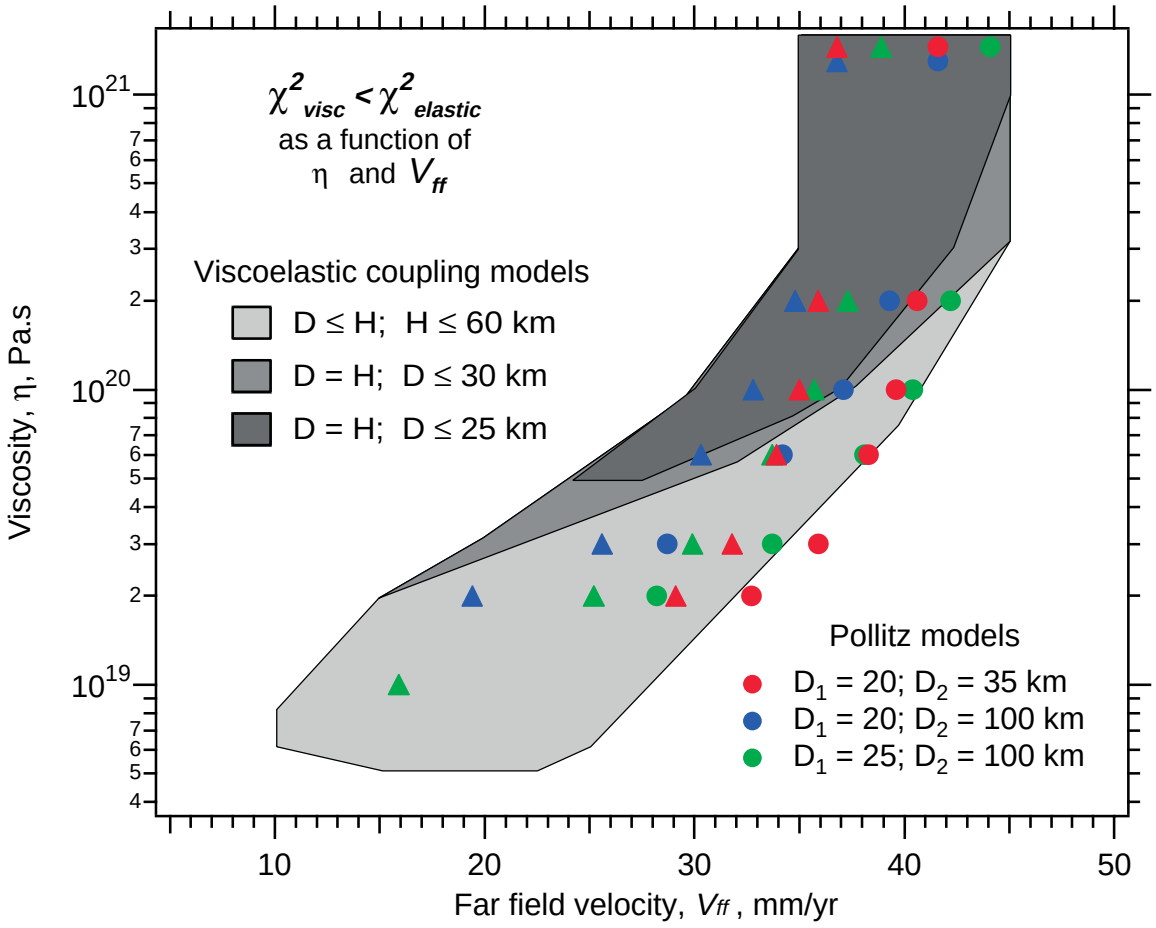


**Figure 7.** The area of light shading shows the range of viscosities and far-field velocities for $D < H$ viscoelastic coupling models that fit the observed velocity profile of Figure 6 as well or better than the elastic model. The medium shading shows the range of solutions for $D = H$ models with $D \leq 30$ km, while the dark shading shows solutions with $D \leq 25$ km. The dots and triangles show the range of solutions using the *Pollitz* [1992] postseismic relaxation model on a spherically stratified Earth, while also solving for interseismic strain accumulation and the reference frame of the velocity data. The dots show solutions with the two northeastern stations omitted, while the triangles show solutions with them included. The different colors are for different elastic and viscoelastic layer thicknesses.

<10% difference between the 1993–1996 and 1996–1998 velocity fields. As η increases above 2–3 × $10^{20}$ Pa s, the viscoelastic solution approaches the elastic case, with $V_{ff}$ of ~40 mm/yr. The viscoelastic models provide very little constraint on locking depth or elastic thickness. A few of the better fitting (lowest reduced $\chi^2$) solutions are given in Table 8, where we show a selection of solutions with $V_{ff}$ < 33 mm/yr, $D \geq 14$ km, and $H < 60$ km. The very best solutions have locking depths <20 km. However, locking depths between 10 and 25 km provide nearly as good fits.

[49] A feature of the viscoelastic models is that there is a velocity maximum some 30–100 km from the fault (e.g., Figure 6). A decreasing velocity with distance from the fault is matched

**Table 8.** Best Viscoelastic Coupling Models With $V_{ff} < 33$ mm/yr, $D \geq 14$ km, and $H \leq 60$ km[a]

| $\eta$, Pa s | $V_{ff}$, mm/yr | $D$, km | $H$, km | $\chi^2$ Ratio[b] |
|---|---|---|---|---|
| | | *D < H Models* | | |
| $1 \times 10^{19}$ | 22.5 | 14 | 60 | 0.79 |
| $2 \times 10^{19}$ | 27.5 | 16 | 60 | 0.78 |
| $2 \times 10^{19}$ | 25.0 | 16 | 45 | 0.80 |
| $2 \times 10^{19}$ | 22.5 | 18 | 40 | 0.81 |
| $3 \times 10^{19}$ | 27.5 | 18 | 45 | 0.80 |
| $4 \times 10^{19}$ | 30.0 | 20 | 45 | 0.79 |
| $4 \times 10^{19}$ | 27.5 | 25 | 35 | 0.82 |
| $5 \times 10^{19}$ | 30.0 | 25 | 35 | 0.80 |
| $6 \times 10^{19}$ | 32.5 | 20 | 35 | 0.80 |
| $8 \times 10^{19}$ | 32.5 | 25 | 30 | 0.80 |
| | | *D = H models* | | |
| $6 \times 10^{19}$ | 30.0 | 25 | - | 0.90 |
| $6 \times 10^{19}$ | 27.5 | 25 | - | 0.93 |
| $8 \times 10^{19}$ | 32.5 | 25 | - | 0.84 |

[a]Strike is 150° and dip is 90° in all models. Recurrence interval is 300 years in all models.
[b]Ratio of reduced $\chi^2$ to the reduced $\chi^2$ of the elastic solution. $\mu = 3 \times 10^{10}$ Pa in all models; this is assumed to be the same in both elastic and viscoelastic layers.

to some extent by the observed velocities at the edges of the networks (Figure 6), particularly to the southwest, but we do not have enough far-field data or low enough uncertainties to be fully confident of this result. We also note that a signal of this sort could arise from a reference frame rotation interacting with a purely elastic fault slip model, and we explore this further in section 4.5.3.

### 4.5.2. Savage and Prescott model: *D = H* formulation

[50] For models with the restriction $D = H$ we perform a similar grid search for acceptable solutions, varying $D$ from 8 to 40 km, $\eta$ from 0.3 to 100 $\times 10^{19}$ Pa s, and $V_{ff}$ from 7.5 to 50 mm/yr. Though some $D > 30$ km solutions are acceptable, we further restrict these models to two cases, $D \leq 30$ km and $D \leq 25$ km, and show the resulting sets of acceptable models in Figure 7. We may summarize our $D = H$ results by saying $\eta > 8 \times 10^{19}$ Pa s and $V_{ff} > 30$ mm/yr for $D = 20$ km, $\eta > 5 \times 10^{19}$ Pa s and $V_{ff} > 25$ mm/yr for $D = 25$ km, and $\eta > 2 \times 10^{19}$ Pa s and $V_{ff} > 15$ mm/yr for $D = 30$ km. The parameters of some of the best fitting models are included in Table 8.

### 4.5.3. Pollitz model

[51] In the previous modeling we used the outer coordinate velocity solution to bring the two 1996–1998 data sets into a reference frame aligned with the assumed azimuth along which slip is accumulating at depth beneath the Philippine Fault. In this section we take a different approach in order to separate the rotation and strike-slip components of the deformation.

[52] We first transform both our 1996–1998 velocities and the *Yu et al.* [1999] 1996–1998 velocities into a PH-fixed reference frame, assuming the PA-PH Euler vector of *Seno et al.* [1993] scaled for NUVEL-1A and using the methodology described in section 2.5. We then project the observed 1996–1998 PH-fixed velocities onto the planar coordinate system and model the resulting velocities, $V_{obs}$, as $V_{obs} = V_{ff} \times V_{steady}(D, \theta, c) + V_{visco}(\eta, D_T, D_B) + V_{trans}(\text{data set}) + V_{rot}(\mathbf{r}, \mathbf{r_0}, \Omega_{\text{data set}})$. $V_{steady}$ is the unit steady state velocity field associated

**Table 9.** Best Fitting Pollitz-Style Viscoelastic Models for Various $\eta$, $D_T$, and $D_B$[a]

| $\eta$, Pa.s | $V_{ff}$,[b] mm/yr | $\Omega$[c] °/Myr | $D_T$, km | $D_B$, km | $\chi^2$ Ratio[d] |
|---|---|---|---|---|---|
| | | *NW Stations, BRG1 and LUZD Included* | | | |
| $3 \times 10^{19}$ | 32 ± 2 | 1.1 ± 0.3 | 20 | 35 | 0.89 |
| $3 \times 10^{19}$ | 26 ± 2 | 1.8 ± 0.3 | 20 | 100 | 0.79 |
| $2 \times 10^{19}$ | 25 ± 2 | 2.0 ± 0.3 | 25 | 100 | 0.80 |
| | | *NW Stations BRG1 and LUZD Excluded* | | | |
| $3 \times 10^{19}$ | 36 ± 2 | 0.6 ± 0.4 | 20 | 35 | 0.95 |
| $6 \times 10^{19}$ | 34 ± 2 | 0.8 ± 0.4 | 20 | 100 | 0.91 |
| $3 \times 10^{19}$ | 34 ± 2 | 1.0 ± 0.4 | 25 | 100 | 0.89 |

[a]Strike is 150°, dip is 90°, and rake is 0° in all models.
[b]Uncertainties in $V_{ff}$ and $\Omega$ are formal 1s errors from least squares inversion, scaled by $\sqrt{\chi^2_R}$.
[c]Rotation rate of Luzon relative to PH, based on PICMP 1996–1998 velocity field.
[d]Ratio of reduced $\chi^2$ to the reduced $\chi^2$ of the corresponding elastic solution. $\mu = 3.6 \times 10^{10}$ Pa in crustal layers, increasing with depth to $7 \times 10^{10}$ Pa in upper mantle.

with interseismic strain accumulation, which we calculate using a standard *Savage and Burford* [1973] model for unit slip rate below locking depth $D$ on an infinitely long fault. It is a function of the locking depth $D$ and the azimuth of the fault, $\theta$, and it scales linearly as the far-field strike-slip velocity $V_{ff}$. We also include a parameter $c$, which is the offset (if any) from the 1990 fault trace of the model fault along which interseismic strain is accumulating. $V_{visco}$ is the velocity field calculated from a *Pollitz* [1992] model, using Model 4a of *Silcock and Beavan* [2001] for the coseismic slip distribution of the 1990 earthquake as input. $V_{visco}$ is a function of the viscosity $\eta$ and the top and bottom depths, $D_T$ and $D_B$, of the viscous layer (where $D_T$ is taken equal to $D$). $V_{trans}$ and $V_{rot}$ are velocities due to translation and rotation of the reference frame. Because the PICMP velocities and *Yu et al.*'s [1999] velocities are not necessarily in the same realization of PH-fixed, $V_{trans}$ and $V_{rot}$ are functions of the data set. $V_{trans}$ takes on a different constant value for each data set, while $V_{rot}$ depends on the position vector of the observation point $\mathbf{r}$, the assumed position of the rotation pole relative to PH $\mathbf{r}_0$, and a different constant rotation rate $\Omega_{data\ set}$ for each data set. For $\mathbf{r}_0$ we choose a position in NE Luzon close to the LUZ-PH pole of *Rangin et al.* [1999], but the derived rotation rate does not depend on the position of the pole; changing the assumed pole position will simply result in a change in the translation components, $V_{trans}$.

[53] This equation is linear in $V_{trans}$, $V_{rot}$, and $V_{ff}$ but nonlinear in $D$, $\theta$, $c$, and $V_{visco}$. We therefore solve it by a mixture of grid search and least squares. We prepare a range of models $V_{steady}$ and $V_{visco}$ with varying values of $D$, $\theta$, $c$, $\eta$, $D_T$, and $D_B$, and then invert each by least squares for the four parameters of $V_{trans}$ (two velocity components for each data set), two parameters of $\Omega_{data\ set}$, and $V_{ff}$. We again deem acceptable models to be those for which the reduced $\chi^2$ of the fit is smaller than the reduced $\chi^2$ for the elastic solution. In this modeling the elastic solution is the one for which $V_{visco} = 0$. It differs slightly from the elastic solution in Table 7 and Figure 6 because of the different parameterization of the reference frame.

[54] In the earlier modeling we removed two points in NW Luzon from the observations because they appeared to be affected by deformation across the Cordillera Central that we were not including in our model. Because these two points may be relevant to *Rangin et al.*'s [1999] hypothesis of rapid rotation of Luzon,

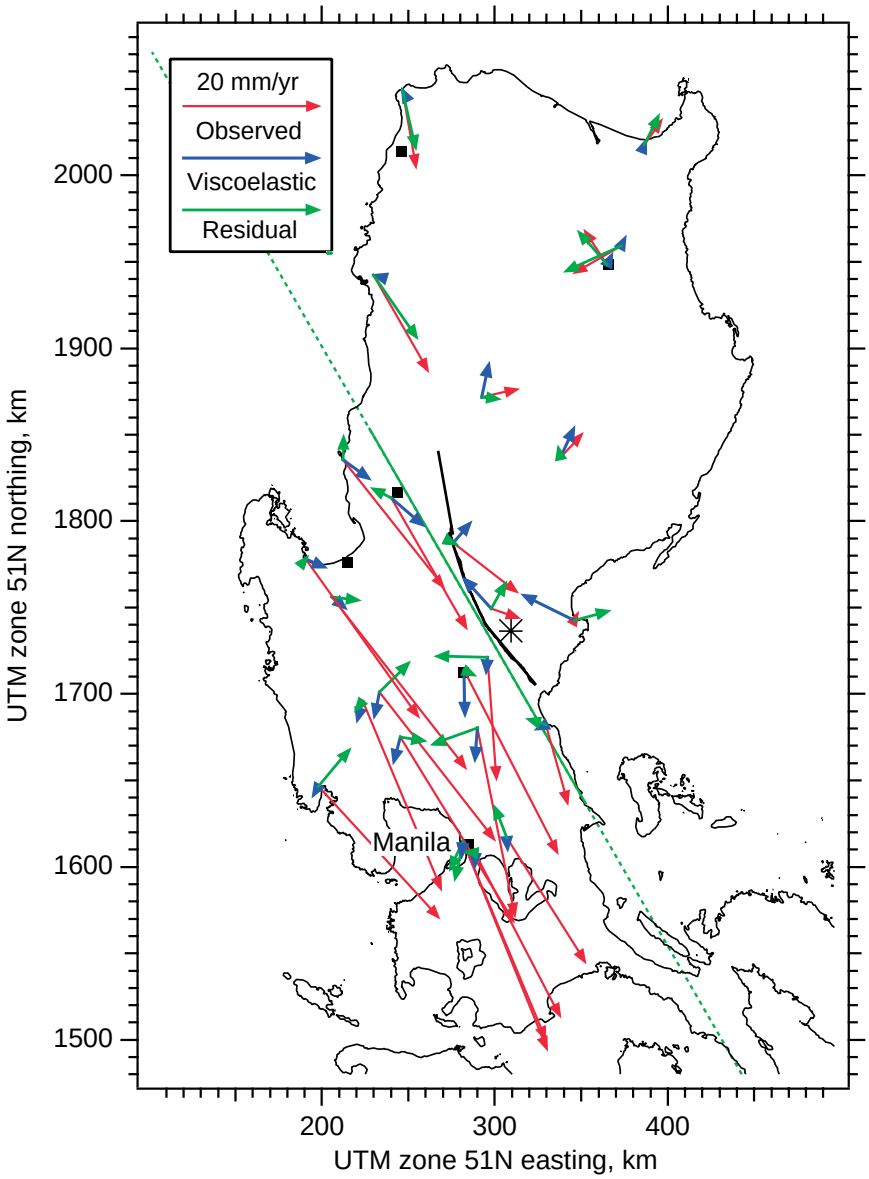


**Figure 8.** An example of a *Pollitz* [1992] viscoelastic solution, specifically, the second entry in Table 9. The red (dark) arrows are the observed velocities with the reference frame rotation and translation applied, so that both the PICMP and *Yu et al.* [1999] velocities are in a NE Luzon-fixed frame. The blue (medium) arrows are the calculated viscoelastic postseismic response averaged over the 1996–1998 interval. The green (light) arrows show the residual velocities after all effects have been modeled. The green line (dashed offshore) shows the surface trace of the model for the steady interseismic velocity field, but the interseismic velocities from this model are not shown in the figure. The black line shows the surface trace of the 1990 rupture model from *Silcock and Beavan* [2001]. Viscoelastic signals of up to 8 mm/yr are present in this solution. Error ellipses, station codes, and most city names are omitted from this figure in order to improve clarity.

we run two sets of models, one with the points included and one with them excluded. We find that $\theta = 150^\circ$ is the best solution for the azimuth of deep interseismic slip in all cases, with the fit worsening markedly when $\theta$ deviates by only a few degrees from this value. Satisfactory solutions for the offset $c$ vary between 0 and 5 km SW of the 1990 surface trace (measured near the 1990 epicenter), very similar to the range of solutions for the purely elastic models shown in Figure 4.

[55] We investigate three geometries for the Pollitz viscoelastic models, one with a viscoelastic lower crust between 20 and 35 km depth and two with a viscoelastic lower crust and upper mantle between 20–100 km and 25–100 km depths. The latter two models consist effectively of an elastic upper crust over a viscoelastic sphere, and we include them to show the effect of varying the thickness of the viscoelastic layer and of varying the depth of transition between elastic and viscoelastic behavior. The results of the inversions are summarized in Table 9 and Figure 6, and one of the best fitting models is shown in Figure 8.

[56] In general, models that fit the data may be summarized as follows: lower viscosities require lower far-field velocities and more rapid rotation of Luzon relative to PH, but there is a lower limit of $V_{ff}$ and $\eta$ (and upper limit of $\Omega$) beyond which the model no longer fits the data.

[57] Including the two NW Luzon stations decreases $V_{ff}$ by ~4 mm/yr and increases $\Omega$ by 0.4°/Myr for the same value of $\eta$, with these differences remaining almost constant over all models. Also, slightly lower $V_{ff}$ and $\eta$ (and higher $\Omega$) solutions are permitted when these stations are included.

[58] The effect of a thick viscoelastic layer compared to a thin viscoelastic channel is that the inferred $V_{ff}$ is smaller, and $\Omega$ is larger, for a given $\eta$. The differences between the solutions increase for smaller values of $\eta$ with $V_{ff}$ decreasing by as much as 10 mm/yr and $\Omega$ increasing by 1.1°/Myr in an extreme case, though generally the differences between the thin and thick viscoelastic layer models are much smaller than this. The minimum allowed $V_{ff}$ for the 20–35 km thin channel model is 29 mm/yr, substantially larger than the minimum $V_{ff}$ in any of our other models.

[59] Most acceptable models have rotation rates of Luzon relative to PH of <1.5°/Myr using our velocities, though at one extreme of acceptable thick viscoelastic layer model (the lowest $V_{ff}$ case with NW Luzon stations included), this rate approaches 3°/Myr. The rotation rates derived from the velocities of *Yu et al.* [1999] are uniformly $1.2^\circ \pm 0.1^\circ$ higher than those for our velocities, suggesting that *Yu et al.*'s [1999] and our realizations of ITRF96 differ by this rotation rate (see also Figure 3b).

## 5. Discussion

### 5.1. Postseismic Deformation and Estimated Viscosity

[60] Surface deformation in the 3–8 years after the earthquake can be described using an elastic model with ~40 mm/yr slip below ~15 km depth on or near the coseismic rupture surface, with no evidence for this rate changing by more than ~10% between 1993–1996 and 1996–1998. In the absence of accelerated postseismic slip or significant viscoelastic relaxation, this implies a long-term slip rate of 40 mm/yr on the Philippine Fault. This high a rate is unlikely for several reasons. It implies a repeat time of about 120–150 years for 6 m displacement earthquakes, yet at least 300–400 years elapsed between the 1645 earthquake and the 1990 event and between the ~1300 event and 1645 [*Daligdig*, 1997]. It is faster than the ~35 mm/

yr rate measured on the fault farther south in Leyte, while we expect from kinematic arguments that the left-lateral rate reduces farther north since some of the slip may be taken up on additional structures present in and adjacent to Luzon, such as the Sibuyan Sea Branch [*Aurelio et al.*, 1998] and the Macolod Corridor [*Rangin et al.*, 1999]. Long-term slip as shallow as 15 km is barely consistent with the 6 m coseismic rupture in 1990 that may have reached 20–25 km depths and appears to have initiated at 25 km depth. None of these is by itself an irresistible argument, but together they suggest that accelerated postseismic deformation is having an important effect on the 1993–1998 velocity observations.

[61] One explanation for the inferred 40 mm/yr rate and 15 km locking depth is continuing slip at higher than the long-term rate on the fault plane below ~15 km depth, with the surrounding medium behaving elastically. This would be particularly plausible if there had been significantly less coseismic slip in the depth range 15–20 km than at shallower levels, and the deeper slip is now "catching up." We cannot completely rule this out, but *Silcock and Beavan*'s [2001] interpretation of the coseismic displacement observations does suggest that slip of magnitude 6 m reaches depths of at least 20 km along a significant part of the 1990 rupture.

[62] An alternative explanation is that coseismic slip was more or less uniform throughout the 0 to 15–20 km depth range, and we are now seeing accelerated deformation due to viscoelastic relaxation of the lower lithosphere. Using *Savage and Prescott*'s [1978] viscoelastic coupling model of the earthquake cycle with locking depths of 10–25 km, elastic layer thicknesses of 25–60 km, and a 300 year recurrence interval, we can fit the velocity data with viscosities >0.5 $\times$ $10^{19}$ Pa s and long-term, far-field velocities >10 mm/yr, where lower viscosities correspond to lower far-field velocities. Long-term velocities of ~20 mm/yr, which correspond on average to 6 m earthquakes every 300 years, require viscosities in the range 0.5–2 $\times$ $10^{19}$ Pa s to fit the observed velocity data. These viscosities correspond to Maxwell times on the order of 5–20 years or ~5% of the typical earthquake recurrence interval.

[63] For viscoelastic coupling models in which the elastic thickness and locking depth are equal we find higher viscosities and far-field velocities. We favor models with $D \leq 25$ km since these depths correspond to the nucleation depth of the 1990 earthquake and to the best estimates of depth of coseismic slip in that earthquake [*Silcock and Beavan*, 2001]. These models lead to viscosities >5 $\times$ $10^{19}$ Pa s and far-field velocities >25 mm/yr, corresponding to a Maxwell time of >50 years or ~15% of the typical earthquake recurrence interval.

[64] Using *Pollitz*'s [1992] model of viscoelastic effects following the 1990 coseismic rupture, we find viscosities >2 $\times$ $10^{19}$ Pa s and far-field velocities >29 mm/yr for the case of a thin (15 km) viscoelastic channel and viscosities >1 $\times$ $10^{19}$ Pa s and far-field velocities >16 mm/yr for the case of a thick viscoelastic layer. To match a far-field velocity (or long-term slip rate) of <30 mm/yr, all our viscoelastic models require lower crustal and/or upper mantle viscosities in the range 1–10 $\times$ $10^{19}$ Pa s, with a preference for the range 2–6 $\times$ $10^{19}$ Pa s.

[65] Previous studies of postseismic effects following large to great strike-slip earthquakes have concentrated on Californian events. Following *Savage and Prescott*'s [1978] paper, *Thatcher* [1983] assembled geodetic data following the 1857 Fort Tejon and 1906 San Francisco earthquakes to try to establish a history of strain throughout an earthquake cycle. While the melding of southern and northern California data in this way has been

challenged [e.g., *Scholz*, 1990], *Thatcher*'s [1983] study remains the best effort to date at generating a complete history for a great strike-slip earthquake cycle. Thatcher found that the strain data could be best fit with a Maxwell time ~10% of the earthquake recurrence interval, assumed to be 150 years in his study. *Li and Rice* [1987], while using a more sophisticated model, found similar values for Maxwell time. *Pollitz and Sacks* [1992] inverted triangulation observations from the 66 years following the 1857 Fort Tejon earthquake using a spherically stratified Earth model. They found the best fits to upper mantle viscosity to be in the range $0.4-0.8 \times 10^{19}$ Pa s, similar to the lowest acceptable estimates from our $D < H$ viscoelastic coupling model and lower than the estimates from our other models. *Savage and Svarc* [1997] found a much higher postseismic than preseismic deformation rate within 30 km of the 1992 Landers rupture, implying a substantial change in deformation rate through the earthquake cycle. Once they had separated out the short-term relaxation signal [*Shen et al.*, 1994], *Savage and Svarc* [1997] could not detect any change in long-term rate during the 3.4 years following the earthquake, implying a relaxation time of 5 years or more. If viscoelastic response is the reason for these observed effects, it implies a lower lithosphere viscosity somewhat smaller than we have estimated in Luzon. *Pollitz et al.* [1998] have attempted to separate viscoelastic and accelerated fault slip mechanisms following the 1989 Loma Prieta earthquake. Though their results are poorly constrained, their best estimate for lower lithosphere viscosity is $\sim 10^{19}$ Pa s, which is also toward the lower end of our Luzon estimates. Our results suggest that lower lithosphere viscosities tend to be lower in California than in northern Luzon, presumably because the geothermal gradient is higher in California.

[66] We should perhaps remark on the ≥45 km elastic thicknesses found in our best fitting $D < H$ viscoelastic models. Given the makeup of the Philippines as accreted island arc terranes and the volcanic activity in southern Luzon, it might be expected that the lithosphere is thinner and hotter than normal continental lithosphere. However, this argument applies better to the southern Philippines, whereas Luzon, particularly northern Luzon, is composed of terranes with attached basement complexes that appear to be of lithospheric thickness [*Karig*, 1983]. The initiation depth of 25 km for the 1990 earthquake also argues against a particularly small elastic thickness. By contrast, it should be recalled (Table 6) that viscoelastic models with elastic thicknesses as small as 25 km provide better fits to the observed velocities than the purely elastic model, even though they do not provide the very lowest residuals (Figure 7). It is possible that the large values of $H$ are the way our simple model attempts to match a more realistic situation in which viscosity depends on temperature and rock type and so varies continuously with depth in the Earth.

### 5.2. Plate Boundary Deformation

[67] The present velocities of points in northeastern Luzon are 0–10 mm/yr westward relative to *Seno et al.*'s [1993] definition of the Philippine Sea Plate (Figure 3b). If these northernmost velocities are unaffected by postseismic deformation following the 1990 earthquake, this implies (Figure 3b) either that there is extension occurring between PH and NE Luzon or that the Euler vector of *Seno et al.* [1993] is slightly underestimating the westward velocity of PH. The first of these possibilities is most unlikely on geological grounds.

[68] If the northernmost velocities are affected by 1990 postseismic deformation, this may be the explanation for the small westward velocities. On the basis of our viscoelastic modeling

(e.g., Figure 6), the maximum additional NW directed velocity in NE Luzon resulting from postseismic deformation is ~5 mm/yr. Assuming the accuracy of the *Seno et al.* [1993] PH Euler vectors, this implies that there is no (±5 mm/yr) convergence taking place between NE Luzon and PH across the East Luzon Trough and the Sierra Madre, suggesting that NE Luzon may be part of the Philippine Sea Plate. (It is perhaps more likely on geological grounds that there is a small component of convergence across the East Luzon Trough and therefore that *Seno et al.*'s [1993] Euler vector is slightly underestimating the westward motion of PH.) These arguments nevertheless support *Hamburger et al.*'s [1983] contention that the primary locus of PH-EU motion is the Manila Trench; the incipient subduction along the East Luzon Trough is not yet taking up more than a small fraction of the motion, or this subduction has been stalled by the arrival of the Benham Plateau at the trench [*Rangin et al.*, 1999]. The results from *Yu et al.*'s [1999] stations in northwestern Luzon suggest up to 10 mm/yr convergence across the Cordillera Central, but this still implies that ~80 ± 5 mm/yr is taken up at or near the Manila Trench at the latitudes of northern Luzon (remembering that the Sunda Plate in this region is moving some 10–15 mm/yr ESE relative to stable Eurasia [*Michel et al.*, 2001]). The high convergence rate across the Manila Trench has also been found in *Rangin et al.*'s [1999] GPS study and in *Kreemer et al.*'s [2000] combined inversion of GPS velocities and seismic strain rates. Paucity of large events at the Manila Trench during the twentieth century implies either largely aseismic subduction or the occurrence of occasional extremely large earthquakes at the trench.

[69] If the PH-EU Euler vector of *Kotake et al.* [1998] is assumed, then points in NE Luzon have a substantial 20 mm/yr southward velocity with respect to the Philippine Sea Plate. There is no tectonic or geological reason to expect such motion, and we take this as evidence of inaccuracy in the *Kotake et al.* [1998] result. This is not surprising because they had available only four GPS points, all in the northern half of the Philippine Sea Plate, to calculate their EU-PH Euler vector. Our results suggest that GPS velocities from northeastern Luzon should be evaluated when assessing the present-day motion of the Philippine Sea Plate, in order to determine whether or not this region is part of the Philippine Sea Plate.

## 6. Conclusions

[70] Between 1993 and 1998 we have detected substantial strike-slip deformation subparallel to the faults that ruptured in the 1990 Luzon earthquake. There is no detectable time dependence in this deformation within the ~10% uncertainties of the velocity estimates. If the observed velocities are interpreted using an elastic half-space model, the measured deformation rate implies a long-term slip rate (or far-field relative velocity) of ~40 mm/yr.

[71] There are several lines of evidence against this high a slip rate. In particular, the long-term rate of earthquake recurrence along the Philippine fault system in central and northern Luzon from paleoseismic data and historical observations, even though relatively poorly documented, suggests that 40 mm/yr is far too high a long-term slip rate.

[72] If the effects of accelerated deformation due to postseismic viscoelastic relaxation in the lower lithosphere are taken into account, the modeled long-term slip rate could be as low as 15–20 mm/yr, in good accord with *Daligdig*'s [1997] paleoseismic data. However, most of our viscoelastic models give faster rates of 20–35 mm/yr, suggesting a possible discrep-

ancy between paleoseismic and geodetic estimates of long-term slip rate.

[73] We infer a lower lithosphere viscosity of $2-6 \times 10^{19}$ Pa s if viscoelastic relaxation is the explanation for the observed postseismic deformation rates. This viscosity implies a Maxwell time of 20–60 years, or 7–20% of the average earthquake recurrence interval. These values of viscosity and Maxwell time are several times larger than estimates deduced following several Californian strike-slip earthquakes [*Thatcher*, 1983; *Li and Rice*, 1987; *Pollitz and Sacks*, 1992; *Savage and Svarc*, 1997; *Pollitz et al.*, 1998].

[74] A network with improved spatial distribution of points in Luzon, monitored even as infrequently as every 5 years over the next 50–100 years, promises to provide better data about the role of viscoelastic relaxation in the strike-slip earthquake cycle than any existing data set (though future data from the region of the similar-sized 1999 Izmit, Turkey, earthquake [*Reilinger et al.*, 2000] will also be valuable, as may data from the region of the much smaller Landers earthquake). In particular, it should be possible to accurately measure temporal slowing and broadening of the strain field.

[75] The tectonics of Luzon are dominated by strike-slip motion along the Philippine fault system, not by rapid (5.5°/Myr) large-scale counterclockwise rotation of Luzon, as has been suggested in a recent paper by *Rangin et al.* [1999] based on very limited GPS data. We estimate that Luzon is rotating counterclockwise at 1°–2°/Myr relative to PH.

[76] There is strong evidence that a large majority of the present-day motion convergence between the Philippine and Sunda Plates at the latitude of Luzon is occurring at the Manila Trench, despite the absence of large twentieth century earthquakes at the trench. No more than a few mm/yr can be occurring at the East Luzon Trough unless the PH-EU Euler vector of *Seno et al.* [1993] is substantially in error.

## Acknowledgments

[77] We thank Mike Bevis for suggesting the occupation of a Philippine-wide GPS network to improve the accuracy of the PGNet survey; Doug Larden for his help in setting up the 1993 measurements; the University NAVSTAR Consortium (UNAVCO), particularly Brennan O'Neill and Oivind Ruud, for support of the 1993 and 1998 GPS measurement campaigns; the NAMRIA surveyors who undertook the 1993 measurements and participated in the 1996 and 1998 campaigns; and PHIVOLCS staff for their participation in the 1996 and 1998 campaigns. We particularly thank Ted Koczynski for his participation in several campaigns and his help in organizing the 1996 campaign. We are grateful to Teruyuki Kato for making available data from the WING GPS site at Manila and Pil-Ho Park for data from the Taejeon station; John Haines and Alessia Maggi for designing and implementing the velocity estimation software, VELFRAME; Des Darby for implementing the nonlinear least squares elastic dislocation inversion software; and Fred Pollitz for making his VISCO1D code freely available (http://www-geology.ucdavis.edu/~pollitz/). We thank Mark Stirling and Kelvin Berryman for their constructive comments on an earlier version of the manuscript, and Jim Savage and Kurt Feigl for their thoughtful and stimulating reviews of the submitted manuscript. We thank the International GPS Service and Scripps Institution of Oceanography for supplying precise GPS orbits. The surveys would not have been possible without the loan of GPS receivers from UNAVCO, Lamont-Doherty Earth Observatory (LDEO), Indiana University, and the Institute of Geological and Nuclear Sciences (GNS). The 1993 measurements were funded by NSF grant EAR89-15622 to Chris Scholz and J.B. at LDEO and a University of South Australia (UniSA) grant to Doug Larden at UniSA. We particularly thank Mike Mayhew for helping arrange the supplemental NSF funding for the 1993 measurements. The 1996 campaign was funded by NSF grants EAR89-15622 to LDEO and EAR93-05180 to Indiana University. The 1998 measurements were supported by NSF grant EAR97-26024 to Indiana University. The figures were prepared using GMT [*Wessel and Smith*, 1998] and Igor (http://www.wavemetrics.com), which was also used for some of the calculations. Analysis and interpretation of the data have been funded by the previously mentioned NSF grants and by NZ Foundation for Research, Science and Technology

contracts CO5811 and CO5X0010. D.M.S. is grateful to the University of South Australia for the award of two periods of study leave, which have greatly assisted the analysis effort. LDEO contribution 6147; GNS contribution 2115.

## References

Abe, K., Seismological aspects of the Luzon, Philippines earthquake of July 16, 1990 (in Japanese), *Bull. Earthquake Res. Inst. Univ. Tokyo*, *65*, 851–873, 1990.

Allen, C. R., Circum-Pacific faulting in the Philippines–Taiwan region, *J. Geophys. Res.*, *67*, 4795–4812, 1962.

Aurelio, M. A., E. Barrier, C. Rangin, and C. Muller, The Philippine fault in the late Cenozoic tectonic evolution of Bondoc–Masbate–N. Leyte area, central Philippines, *J. SE Asian Earth Sci.*, *6*(3/4), 221–238, 1991.

Aurelio, M. A., W. F. W. Simons, R. L. Almeda, and the EC-Philippine GPS Team, Present-day plate motions in the Philippines: Interpretation of GPS results of GEODYSSEA, in *The Geodynamics of S and SE Asia (GEODYSSEA) Project*, edited by P. Wilson and G. W. Michel, *Sci. Tech. Rep. STR98/14*, pp. 251–263, GeoForschungsZentrum, Potsdam, Germany, 1998.

Barrier, E., P. Huchon, and M. Aurelio, Philippine fault: A key for Philippine kinematics, *Geology*, *19*, 32–35, 1991.

Beavan, J., M. Moore, C. Pearson, M. Henderson, B. Parsons, S. Bourne, P. England, R. Walcott, G. Blick, D. Darby, and K. Hodgkinson, 1994–1998 deformation within the oblique continental collision zone in the central Southern Alps, New Zealand: Implications for seismic potential of the Alpine fault, *J. Geophys. Res.*, *104*(B11), 25,233–25,255, 1999.

Bibby, H. M., Unbiased estimate of strain from triangulation data using the method of simultaneous reduction, *Tectonophysics*, *82*(1–2), 161–174, 1982.

Bischke, R. E., J. Suppe, and R. del Pilar, A new branch of the Philippine fault system as observed from aeromagnetic and seismic data, *Tectonophysics*, *183*, 243–264, 1990.

Boucher, C., Z. Altamimi, and P. Sillard, Results and analysis of the ITRF96, *IERS Tech. Note 24*, Obs. de Paris, Paris, 1998.

Bowin, C., R. S. Lu, C.-S. Lee, and H. Schouten, Plate convergence and accretion in the Taiwan–Luzon region, *Am. Assoc. Pet. Geol. Bull.*, *62*, 1645–1672, 1978.

Bureau of Mines and Geosciences, *Geology and Mineral Resources of the Philippines*, vol. 1, *Geology*, 406 pp., Minist. of Nat. Resour., Manila, 1982.

Cardwell, R. K., B. L. Isacks, and D. E. Karig, The spatial distribution of earthquakes, focal mechanism solutions, and subducted lithosphere in the Philippine and northeastern Indonesian islands, in *The Tectonic and Geologic Evolution of Southeast Asian Seas and Islands, Geophys. Monogr. Ser.*, vol. 23, edited by D. Hayes et al., pp. 1–35, AGU, Washington, D. C., 1980.

Chen, Z., B. C. Burchfiel, Y. Liu, R. W. King, L. H. Royden, W. Tang, E. Wang, J. Zhao, and X. Zhang, Global Positioning System measurements from eastern Tibet and their implications for India/Eurasia intercontinental deformation, *J. Geophys. Res.*, *105*(B7), 16,215–16,228, 2000.

Chinnery, M. A., The deformation of the ground around surface faults, *Bull. Seismol. Soc. Am.*, *50*, 355–372, 1961.

Cohen, S. C., Numerical models of crustal deformation in seismic zones, *Adv. Geophys.*, *41*, 133–231, 1999.

Crook, C. N., ADJCOORD: A Fortran program for survey adjustment and deformation modelling, *N. Z. Geol. Surv. Earth Deformation Sect. Rep. 138*, 22 pp., Dep. Sci. Indust. Res., Lower Hutt, New Zealand, 1992.

Daligdig, J. A., Recent faulting and paleoseismicity along the Philippine fault zone, north central Luzon, Philippines, Ph.D. thesis, Fac. of Sci., Kyoto University, 1997.

Darby, D. J., and J. Beavan, Evidence from GPS measurements for contemporary interplate coupling on the southern Hikurangi subduction thrust and for partitioning of strain in the upper plate, *J. Geophys. Res.*, in press, 2001.

DeMets, C., R. G. Gordon, D. F. Argus, and S. Stein, Effect of recent revisions to the geomagnetic reversal time scale on estimates of current plate motions, *Geophys. Res. Lett.*, *21*, 2191–2194, 1994.

Dennis, J. E., D. M. Gay, and R. E. Welsch, An adaptive non-linear least-squares algorithm, *ACM Trans. Math. Software*, *7*, 348–368, 1981a.

Dennis, J. E., D. M. Gay, and R. E. Welsch, Algorithm 573 NL2SOL — An adaptive non-linear least-squares algorithm [E4], *ACM Trans. Math. Software*, *7*, 369–383, 1981b.

Dixon, T. H., M. Miller, F. Farina, H. Wang, and D. Johnson, Present-day motion of the Sierra Nevada block and some tectonic implications for the Basin and Range province, North American Cordillera, *Tectonics*, *19*, 1–24, 2000.

Dusquenoy, T., Contribution de la géodésie à l'étude de grand décrochements actifs associés à des zones de subduction à convergence oblique, Exemple de la grand faille de Sumatra et de la faille Philippine, thesis, Univ. de Paris Sud, Orsay, France, 1997.

Duquesnoy, T., E. Barrier, M. Kasser, M. Aurelio, R. Gaulon, R. S. Punongbayan, and C. Rangin, Detection of creep along the Philippine fault: First results of geo-

detic measurements on Leyte Island, central Philippines, *Geophys. Res. Lett.*, *21*, 975–978, 1994.

Fitch, T. J., Plate convergence, transcurrent faults, and internal deformation adjacent to southeast Asia and the western Pacific, *J. Geophys. Res.*, *77*, 4432–4460, 1972.

Fuller, M., R. McCabe, I. S. Williams, J. Almasco, R. Y. Encina, A. S. Zanoria, and J. A. Wolfe, Paleomagnetism of Luzon, in *The Tectonic and Geologic Evolution of Southeast Asian Seas and Islands: Part 2, Geophys. Monogr. Ser.*, vol. 27, edited by D. Hayes et al., pp. 79–94, AGU, Washington, D. C., 1983.

Hall, R., Reconstructing Cenozoic SE Asia, in *Tectonic Evolution of Southeast Asia*, edited by R. Hall and D. Blundell, *Geol. Soc. Spec. Publ.*, *106*, 153–184, 1996.

Hamburger, M. W., R. K. Cardwell, and B. L. Isacks, Seismotectonics of the northern Philippine island arc, in *The Tectonic and Geologic Evolution of Southeast Asian Seas and Islands: Part 2, Geophys. Monogr. Ser.*, vol. 27, edited by D. Hayes et al., pp. 1–22, AGU, Washington, D. C., 1983.

Heki, K., Horizontal and vertical crustal movements from three-dimensional very long baseline interferometry kinematic reference frame: Implication for the reversal timescale revision, *J. Geophys. Res.*, *101*, 3187–3198, 1996.

Hirano, S., T. Nakata, and A. Sangawa, Fault topography and Quaternary faulting along the Philippine fault zone, central Luzon, Philippines, *J. Geogr.*, *95*, 71–93, 1986.

International Seismological Centre, Bulletin of the International Seismological Centre, Newbury, Berkshire, England, U.K., 1992.

Karig, D. E., Plate convergence between the Philippines and the Ryukyu Islands, *Mar. Geol.*, *14*, 153–168, 1973.

Karig, D. E., Accreted terranes in the northern part of the Philippine archipelago, *Tectonics*, *2*, 211–236, 1983.

Kotake, Y., T. Kato, S. Miyazaki, and A. Sengoku, Relative motion of the Philippine Sea plate derived from GPS observations and tectonics of the south-western Japan (in Japanese with English abstract), *J. Seismol. Soc. Jpn.*, *51*(2), 171–180, 1998.

Kouba, J., and Y. Mireault, Analysis Coordinator Report, in *IGS 1996 Annual Report*, edited by J. F. Zumberge, D. E. Fulton, and R. E. Neilan, pp. 55–100, Jet Propul. Lab., Calif. Inst. of Technol., Pasadena, Calif., 1997.

Kreemer, C., W. E. Holt, S. Goes, and R. Govers, Active deformation in eastern Indonesia and the Philippines from GPS and seismicity data, *J. Geophys. Res.*, *105*(B1), 663–680, 2000.

Larson, K. M., J. Freymueller, and S. Philipsen, Global plate velocities from the Global Positioning System, *J. Geophys. Res.*, *102*(B5), 9961–9981, 1997.

Lewis, S. D., and D. E. Hayes, The tectonics of northward propagating subduction along Eastern Luzon, Philippine Islands, in *The Tectonic and Geologic Evolution of Southeast Asian Seas and Islands: Part 2, Geophys. Monogr. Ser.*, vol. 27, edited by D. Hayes et al., pp. 57–78, AGU, Washington, D. C., 1983.

Lewis, S. D., and D. E. Hayes, Plate convergence and deformation, North Luzon ridge, Philippines, *Tectonophysics*, *168*, 221–237, 1989.

Li, V. C., and J. R. Rice, Crustal deformation in great California earthquake cycles, *J. Geophys. Res.*, *92*(B11), 11,533–11,551, 1987.

McCabe, R., J. Almasco, and W. Diegor, Geologic and paleomagnetic evidence for a possible Miocene collision in western Panay, central Philippines, *Geology*, *10*, 325–329, 1982.

McCaffrey, R., Slip partitioning at convergent plate boundaries of SE Asia, in *Tectonic Evolution of Southeast Asia*, edited by R. Hall and D. Blundell, *Geol. Soc. Spec. Publ.*, *106*, 3–18 1996.

Michel, G. W., Y. Q. Yu, S. Y. Zhu, C. Reigber, M. Becker, E. Reinhart, W. Simons, B. Ambrosius, C. Vigny, N. Chamot-Rooke, X. Le Pichon, P. Morgan, and S. Matheussen, Crustal motion and block behaviour in SE-Asia from GPS measurements, *Earth. Planet. Sci. Lett.*, *187*, 239–244, 2001.

Morante, E. M., The Ragay Gulf earthquake of March 17, 1973, southern Luzon, Philippines, *J. Geol. Soc. Philippines*, *28*(2), 69–93, 1974.

Morante, E. M., and C. R. Allen, Displacement on the Philippine fault during the Ragay Gulf earthquake of March 17, 1973 (abstract), *Geol. Soc. Am. Abstr. Programs*, *5*, 744–745, 1973.

Murphy, R. W., The Manila trench–west Taiwan fold belt: A flipped subduction zone?, *Geol. Soc. Malaysia Bull.*, *6*, 27–42, 1973.

Nakata, T., H. Tsutsumi, R. S. Punongbayan, R. E. Rimando, J. Daligdig, and A. Daag, Surface faulting associated with the Philippine earthquake of 1990 (in Japanese), *J. Geogr.*, *99*, 95–112, 1990.

Nakata, T., H. Tsutsumi, R. S. Punongbayan, R. E. Rimando, J. A. Daligdig, A. S. Daag, and G. M. Besana, Surface fault ruptures of the 1990 Luzon earthquake, Philippines, *Spec. Publ. 25*, 92 pp., Res. Cent. for Reg. Geogr., Hiroshima Univ., 1996.

Newhall, C. G., R. V. Sharp, G. F. Wieczorek, L. Wennerberg, and J. Bicknell, The July 16, 1990, Luzon earthquake, Final report to U.S. AID from USGS and PHIVOLCS, U.S. Geol. Surv., Menlo Park, Calif., Oct. 29, 1990.

Nur, A., and G. Mavko, Postseismic viscoelastic rebound, *Science*, *175*, 885–887, 1974.

Okada, Y., Surface deformation due to shear and tensile faults in a half-space, *Bull. Seismol. Soc. Am.*, *75*, 1135–1154, 1985.

Philippine Bureau of Mines, Geological map of the Philippines, scale 1:1,000,000, 9 sheets, Manila, 1963.

Pollitz, F. F., Postseismic relaxation theory on the spherical Earth, *Bull. Seismol. Soc. Am.*, *82*, 422–453, 1992.

Pollitz, F. F., and I. S. Sacks, Modeling of postseismic relaxation following the great 1857 earthquake, southern California, *Bull. Seismol. Soc. Am.*, *82*, 454–480, 1992.

Pollitz, F. F., R. Bürgmann, and P. Segall, Joint estimation of afterslip rate and postseismic relaxation following the 1989 Loma Prieta earthquake, *J. Geophys. Res.*, *103*(B11), 26,975–26,992, 1998.

Prescott, W. H., The determination of displacement fields from geodetic data along a strike slip fault, *J. Geophys. Res.*, *86*(B7), 6067–6072, 1981.

Rangin, C., X. LePichon, S. Mazzotti, M. Pubellier, N. Chamot-Rooke, M. Aurelio, A. Walpersdorf, and R. Quebral, Plate convergence measured by GPS across the Sundaland/Philippine Sea Plate deformed boundary: The Philippines and eastern Indonesia, *Geophys. J. Int.*, *139*, 296–316, 1999.

Reilinger, R. E., et al., Coseismic and postseismic fault slip for the 17 August 1999, M = 7.5, Izmit, Turkey earthquake, *Science*, *289*, 1519–1524, 2000.

Rothacher, M., and L. Mervart (Eds.), *Documentation of the Bernese GPS Software Version 4.0*, 418 pp., Astron. Inst., Univ. of Bern, Bern, Switzerland, 1996.

Rowlett, H., and J. Kelleher, Evolving seismic and tectonic patterns along the western margin of the Philippine Sea plate, *J. Geophys. Res.*, *81*, 3518–3524, 1976.

Savage, J. C., Equivalent strike-slip earthquake cycles in half-space and lithosphere-asthenosphere Earth models, *J. Geophys. Res.*, *95*, 4873–4879, 1990.

Savage, J. C., and R. O. Burford, Accumulation of tectonic strain in California, *Bull. Seismol. Soc. Am.*, *60*, 1877–1896, 1970.

Savage, J. C., and R. O. Burford, Geodetic determination of relative plate motion in central California, *J. Geophys. Res.*, *78*, 832–845, 1973.

Savage, J. C., and M. Lisowski, Viscoelastic coupling model of the San Andreas fault along the big bend, southern California, *J. Geophys. Res.*, *103*, 7281–7292, 1998.

Savage, J. C., and W. H. Prescott, Asthenosphere readjustment and the earthquake cycle, *J. Geophys. Res.*, *83*, 3369–3376, 1978.

Savage, J. C., and J. L. Svarc, Postseismic deformation associated with the 1992 $M_w$ = 7.3 Landers earthquake, southern California, *J. Geophys. Res.*, *102*(B4), 7565–7577, 1997.

Scholz, C. H., *The Mechanics of Earthquakes and Faulting*, 439 pp., Cambridge Univ. Press, New York, 1990.

Seno, T., S. Stein, and A. E. Gripp, A model for the motion of the Philippine Sea plate consistent with NUVEL-1 and geological data, *J. Geophys. Res.*, *98*(B10), 17,941–17,948, 1993.

Shen, Z.-K., D. D. Jackson, Y. Feng, M. Cline, M. Kim, P. Fang, and Y. Bock, Postseismic deformation following the Landers earthquake, California, 28 June 1992, *Bull. Seismol. Soc. Am.*, *84*, 780–791, 1994.

Shen, Z.-K., C. Zhao, A. Yin, Y. Li, D. D. Jackson, P. Fang, and D. Dong, Contemporary crustal deformation in east Asia constrained by Global Positioning System measurements, *J. Geophys. Res.*, *105*(B3), 5721–5734, 2000.

Silcock, D. M., and J. Beavan, Geodetic constraints on coseismic rupture during the 1990 $M_s$ 7.8 Luzon, Philippines, earthquake, *Geochem. Geophys. Geosyst.*, vol. 2, Paper number 2000GC000101 [6979 words, 3 figures, 1 table]. Published July 31, 2001.[Available at http://www.g-cubed.org/publicationsfinal/articles/2000GC000101/fs2000GC000101.html]

Thatcher, W., Nonlinear strain buildup and the earthquake cycle on the San Andreas fault, *J. Geophys. Res.*, *88*(B7), 5893–5902, 1983.

Thibault, C. A., GPS measurements of crustal deformation in the northern Philippine island arc, M.Sc. thesis, 126 pp., Indiana Univ., Bloomington, Indiana, 1999.

Tregoning, P., K. Lambeck, A. Stolz, P. J. Morgan, S. C. McClusky, P. van der Beek, H. McQueen, R. J. Jackson, R. P. Little, A. Laing, and B. Murphy, Determination of current plate motions in Papua New Guinea from Global Positioining System observations, *J. Geophys. Res.*, *103*(B6), 12,181–12,205, 1998.

Wessel, P., and W. H. F. Smith, New, improved version of Generic Mapping Tools released, *Eos Trans. AGU*, *79*(47), 579, 1998.

Yoshida, Y., and K. Abe, Source mechanism of the Luzon, Philippines earthquake of July 16, 1990, *Geophys. Res. Lett.*, *19*, 545–548, 1992.

Yu, S.-B., L.-C. Kuo, R. S. Punongbayan, and E. G. Ramos, GPS observations of crustal deformation in the Taiwan–Luzon region, *Geophys. Res. Lett.*, *26*, 923–926, 1999.

Zhang, J., Y. Bock, H. Johnson, P. Fang, S. Williams, J. Genrich, S. Wdowinski, and J. Behr, Southern California Permanent GPS Geodetic Array: Error analysis of daily position estimates and site velocities, *J. Geophys. Res.*, *102*(B8), 18,035–18,055, 1997.